

## Electronic Supplementary Information

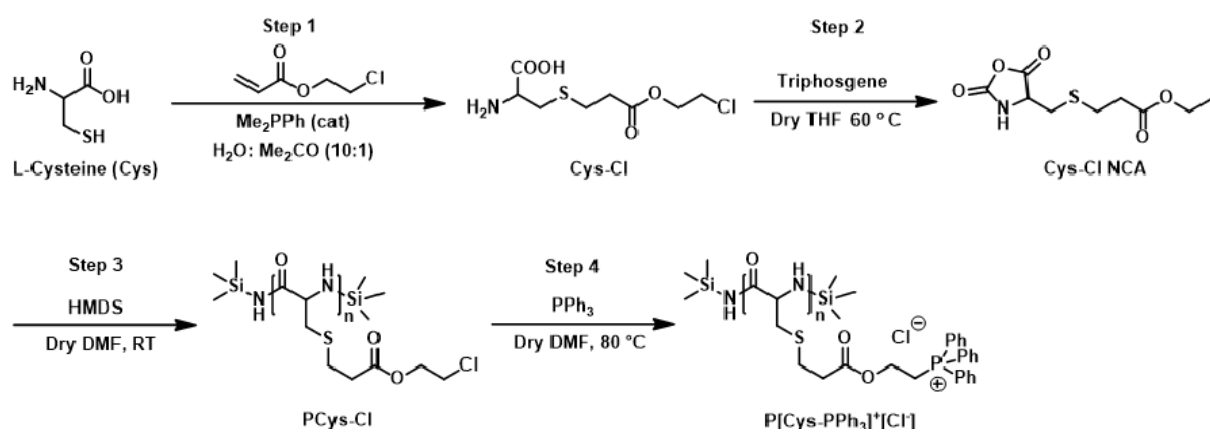
### **Anion-Induced Thermoresponsiveness in Cationic Polycysteine and DNA Binding**

Mahammad Anas, Priyanka Dinda, Mahuya Kar and Tarun K. Mandal\*

*School of Chemical Sciences, Indian Association for the Cultivation of Science, Jadavpur,  
Kolkata 700032, India*

<b>Contents</b>	<b>Page No.</b>
Scheme S1. Synthesis scheme for PCys-Cl and P[Cys-PPh <sub>3</sub> ] <sup>+</sup> [Cl <sup>-</sup> ]	S3
Figure S1. FTIR spectra of all the compounds	S4
Figure S2. ESI-MS spectrum of 2-BrEt-Ac	S5
Figure S3. <sup>1</sup> H-NMR spectrum of 2-BrEt-Ac	S6
Figure S4. <sup>13</sup> C-NMR spectra of 2-BrEt-Ac, Cys-Br, Cys-Br NCA and PCys-Br-1	S7
Figure S5. ESI-MS spectrum of Cys-Br	S8
Figure S6. <sup>1</sup> H-NMR spectrum of Cys-Br	S9
Figure S7. ESI-MS spectrum of Cys-Cl	S10
Figure S8. <sup>1</sup> H-NMR spectra of Cys-Cl, Cys-Cl NCA, PCys-Cl, P[Cys-PPh <sub>3</sub> ] <sup>+</sup> [Cl <sup>-</sup> ]	S11
Figure S9. ESI-MS spectrum of Cys-Br NCA	S12
Figure S10. <sup>1</sup> H-NMR spectrum of Cys-Br NCA	S13
Figure S11. MALDI-TOF-MS of Cys-Cl NCA	S14
Figure S12. <sup>1</sup> H-NMR spectrum of PCys-Br-1	S15
Figure S13. <sup>1</sup> H-NMR spectrum of P[Cys-PPh <sub>3</sub> ] <sup>+</sup> [Br <sup>-</sup> ]-1	S16
Figure S14. <sup>31</sup> P-NMR spectrum of P[Cys-PPh <sub>3</sub> ] <sup>+</sup> [Br <sup>-</sup> ]-1	S17
Figure S15. <sup>1</sup> H-NMR spectrum of P[Cys-PPh <sub>3</sub> ] <sup>+</sup> [Br <sup>-</sup> ]-2	S18
Figure S16. UV-Vis absorption spectra of neat ctDNA and Calibration curve	S19
Figure S17. Zeta potential distribution of P[Cys-PPh <sub>3</sub> ] <sup>+</sup> [Br <sup>-</sup> ]-1	S20
Figure S18. MALDI-TOF-MS of PCys-Br-1	S21

Figure S19.	SEC traces of PCys-Br-1, P[Cys-PPh <sub>3</sub> ] <sup>+</sup> [Br <sup>-</sup> ]-1 and P[Cys-PPh <sub>3</sub> ] <sup>+</sup> [Br <sup>-</sup> ]-1	S22
Figure S20.	CD spectra of PCys-Br-1 and P[Cys-PPh <sub>3</sub> ] <sup>+</sup> [Br <sup>-</sup> ]-1	S23
Figure S21.	TEM image of P[Cys-PPh <sub>3</sub> ] <sup>+</sup> [Br <sup>-</sup> ]-1	S24
Table S1.	Particle size of anion induced P[Cys-PPh <sub>3</sub> ] <sup>+</sup> [Br <sup>-</sup> ]-1 aggregates	S25
Figure S22.	FESEM images of P[Cys-PPh <sub>3</sub> ] <sup>+</sup> [Br <sup>-</sup> ]-1 in presence of anions	S26
Figure S23.	Heating/cooling cycles vs % transmittance plot	S27
Figure S24.	Temperature dependent $D_h$ variation of P[Cys-PPh <sub>3</sub> ] <sup>+</sup> [Br <sup>-</sup> ]-1 aggregates	S28
Figure S25.	Turbidity plot of P[Cys-PPh <sub>3</sub> ] <sup>+</sup> [Br <sup>-</sup> ]-2 solution with SCN <sup>-</sup>	S29
Figure S26.	Turbidity plot of P[Cys-PPh <sub>3</sub> ] <sup>+</sup> [Br <sup>-</sup> ] and P[Cys-PPh <sub>3</sub> ] <sup>+</sup> [Cl <sup>-</sup> ] with BF <sub>4</sub> <sup>-</sup>	S30
Figure S27.	Turbidity plots of P[Cys-PPh <sub>3</sub> ] <sup>+</sup> [Br <sup>-</sup> ]-1 vs. polypeptide concentration	S31
Figure S28.	Turbidity plots of P[Cys-PPh <sub>3</sub> ] <sup>+</sup> [Br <sup>-</sup> ]-1 vs. anion concentration	S32
Figure S29.	Turbidity plot of P[Cys-PPh <sub>3</sub> ] <sup>+</sup> [Br <sup>-</sup> ]-1 in presence of SDS	S33
Scheme S2.	Polyplex formation of P[Cys-PPh <sub>3</sub> ] <sup>+</sup> [Br <sup>-</sup> ]-1 with ctDNA	S34
Figure S30.	The cell viability of KB cells with P[Cys-PPh <sub>3</sub> ] <sup>+</sup> [Br <sup>-</sup> ]-1	S35
Figure S31.	Titration plot of P[Cys-PPh <sub>3</sub> ] <sup>+</sup> [Br <sup>-</sup> ]-1 solution in presence of ctDNA	S36
Figure S32.	Optical spectra of neat EtBr and EtBr-ctDNA intercalated complex	S37
Figure S33.	Photographs of the ctDNA-EtBr complex with P[Cys-PPh <sub>3</sub> ] <sup>+</sup> [Br <sup>-</sup> ]-1	S38
Figure S34.	Emission spectra of P[Cys-PPh <sub>3</sub> ] <sup>+</sup> /ctDNA vs NaCl concentration	S39



**Scheme S1.** Synthesis scheme for PCys-Cl and its cationization to  $\text{P}[\text{Cys-PPh}_3]^+\text{[Cl}^-]$

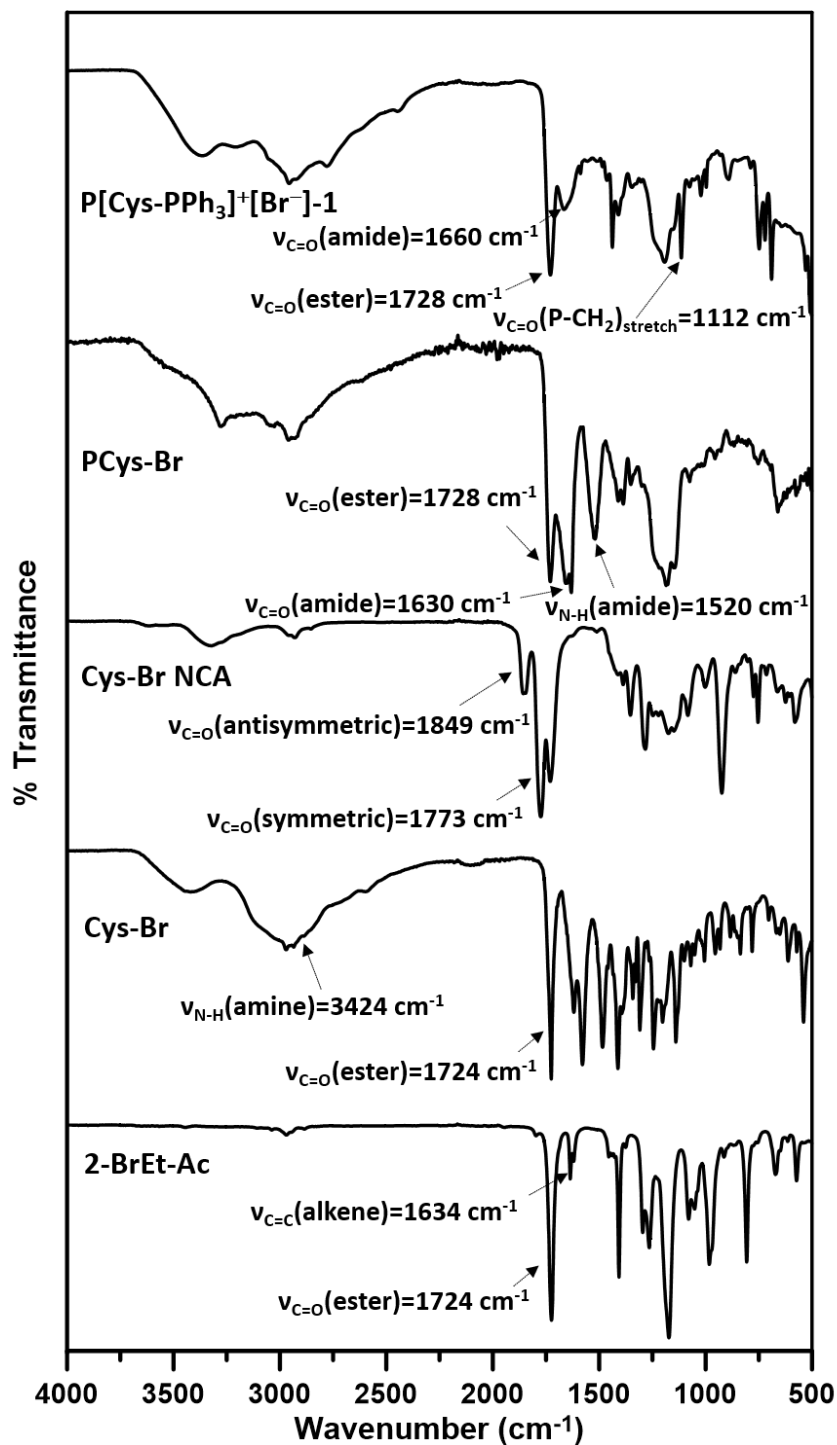


**Figure S1.** FT-IR spectra of all the as-synthesized compounds.

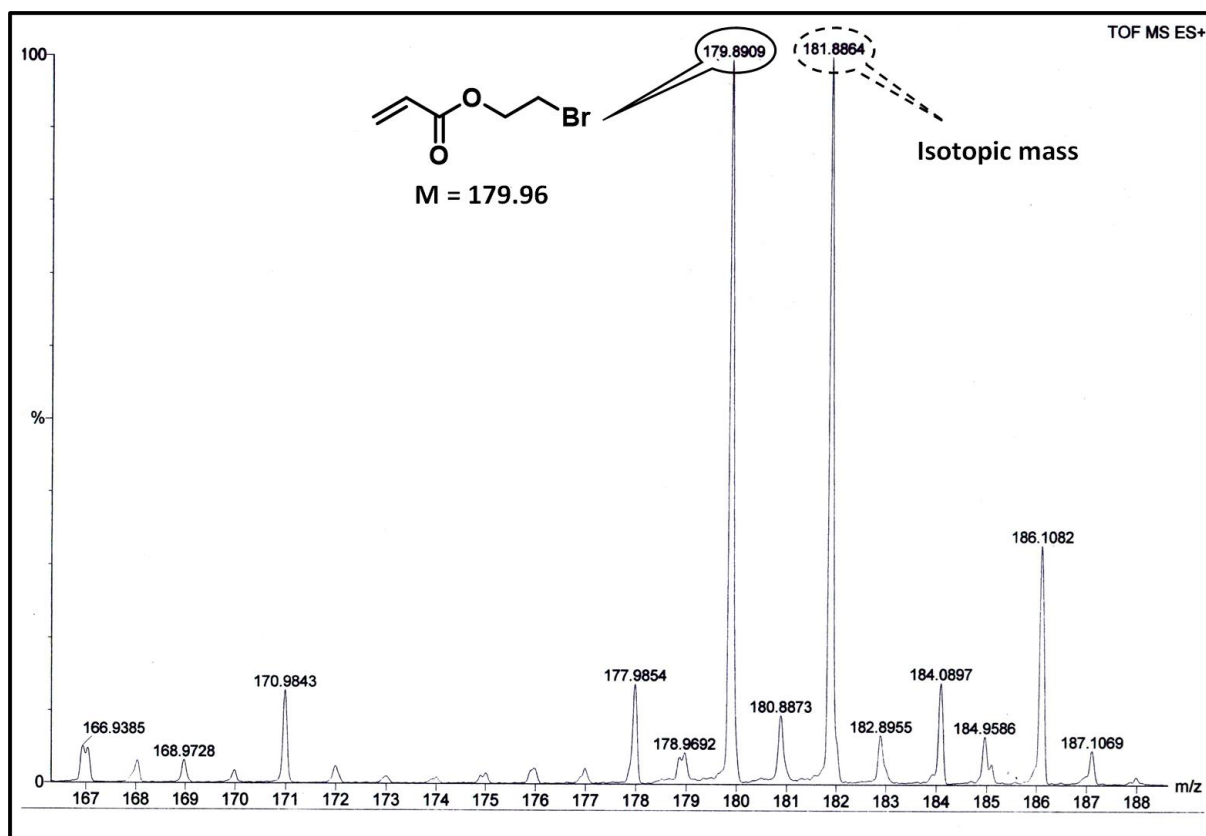


**Figure S2.** ESI-MS spectrum of 2-BrEt-Ac in DCM.

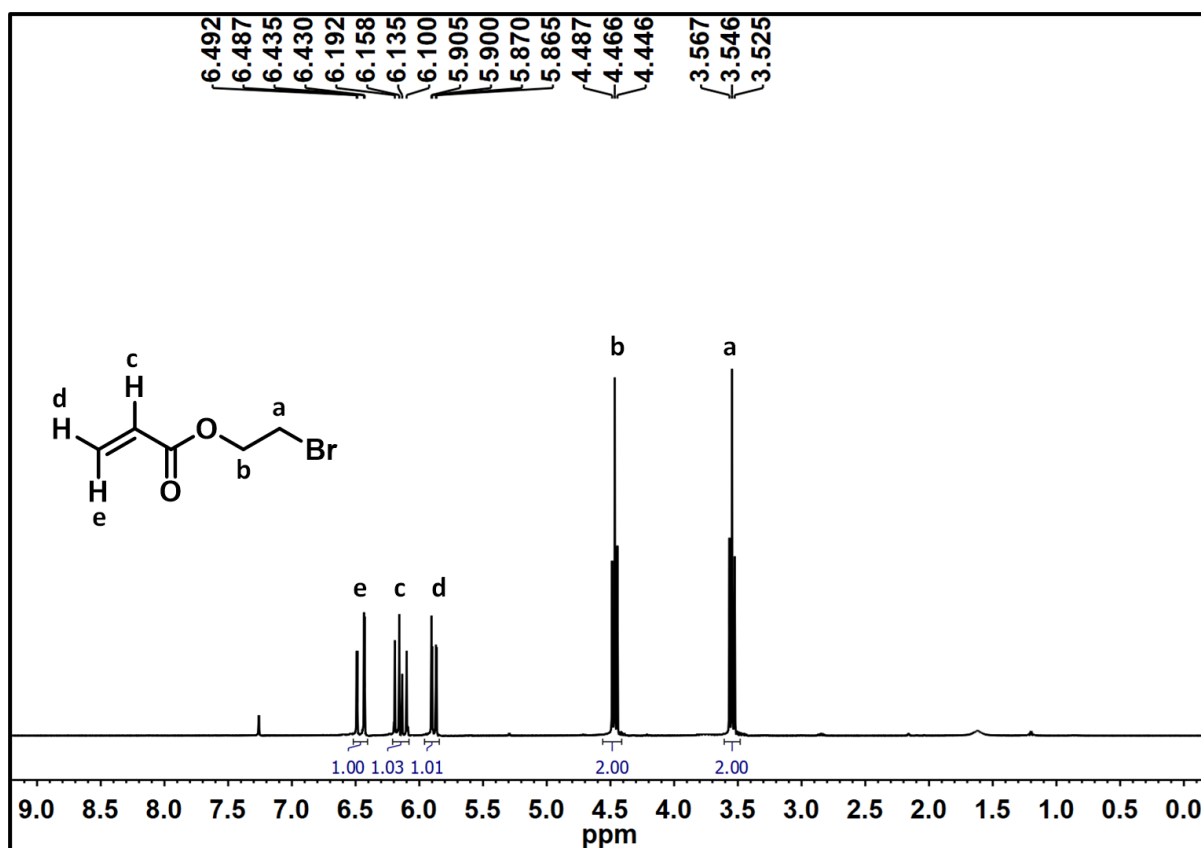


**Figure S3.** <sup>1</sup>H-NMR spectrum of 2-BrEt-Ac in CDCl<sub>3</sub>.

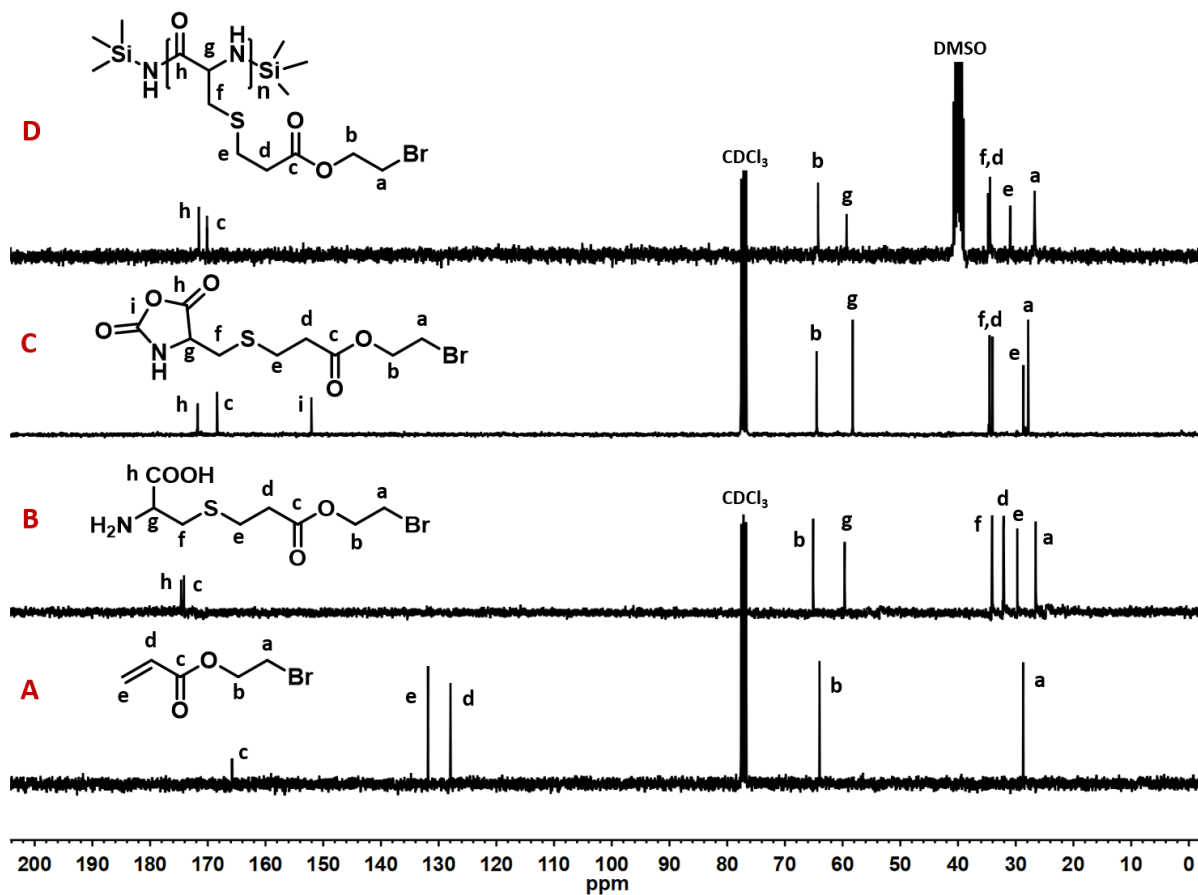


**Figure S4.**  $^{13}\text{C}$ -NMR spectra of 2-BrEt-Ac in  $\text{CDCl}_3$  (A), Cys-Br in  $\text{D}_2\text{O}$  (B), Cys-Br NCA in  $\text{CDCl}_3$  (C) and PCys-Br-1 in  $\text{DMSO-d}_6$  (D).

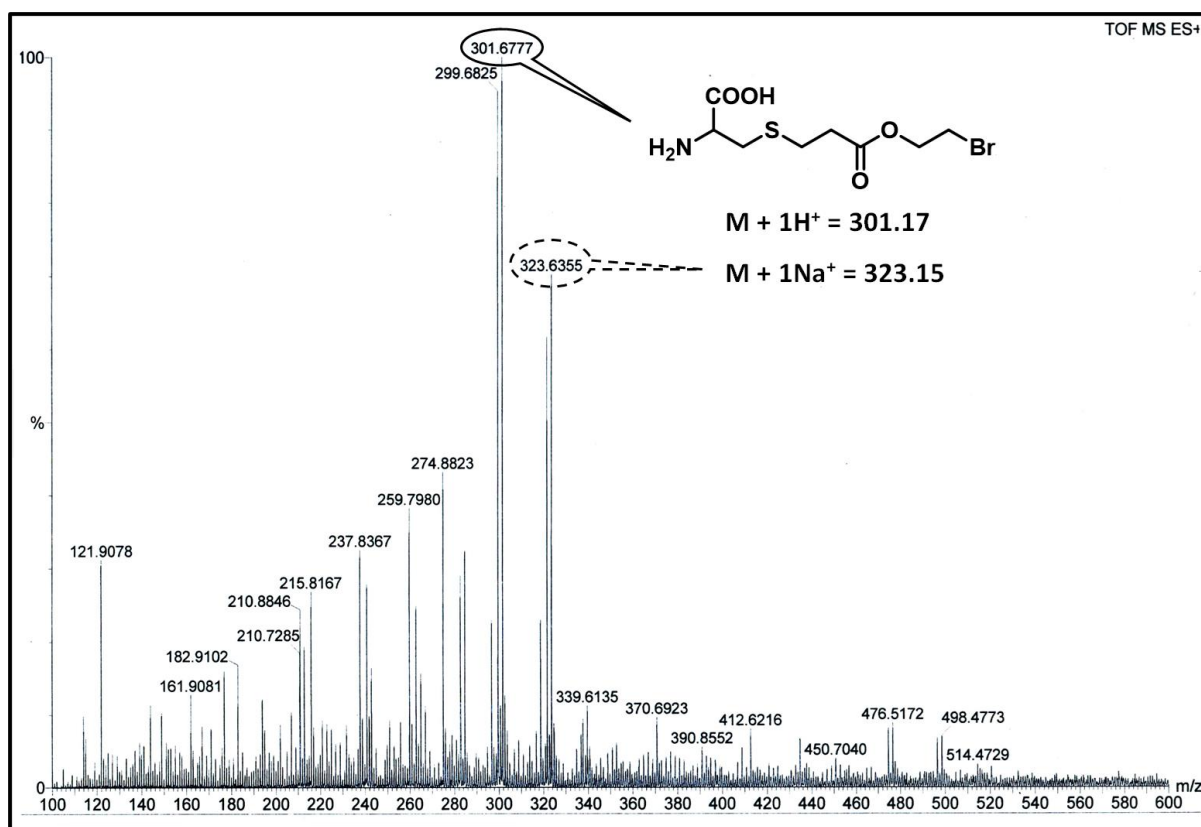


**Figure S5.** ESI-MS spectrum of Cys-Br in H<sub>2</sub>O: MeOH (1:1) mixture.



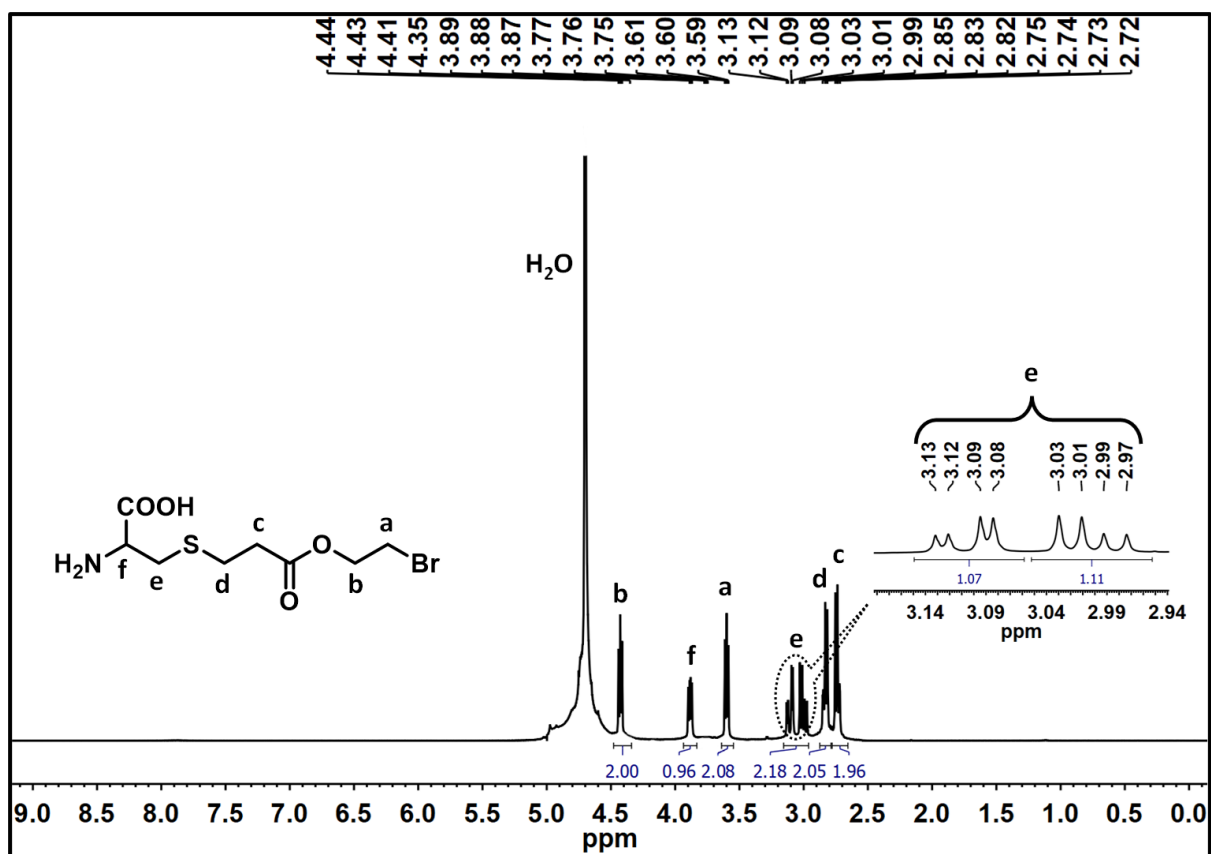
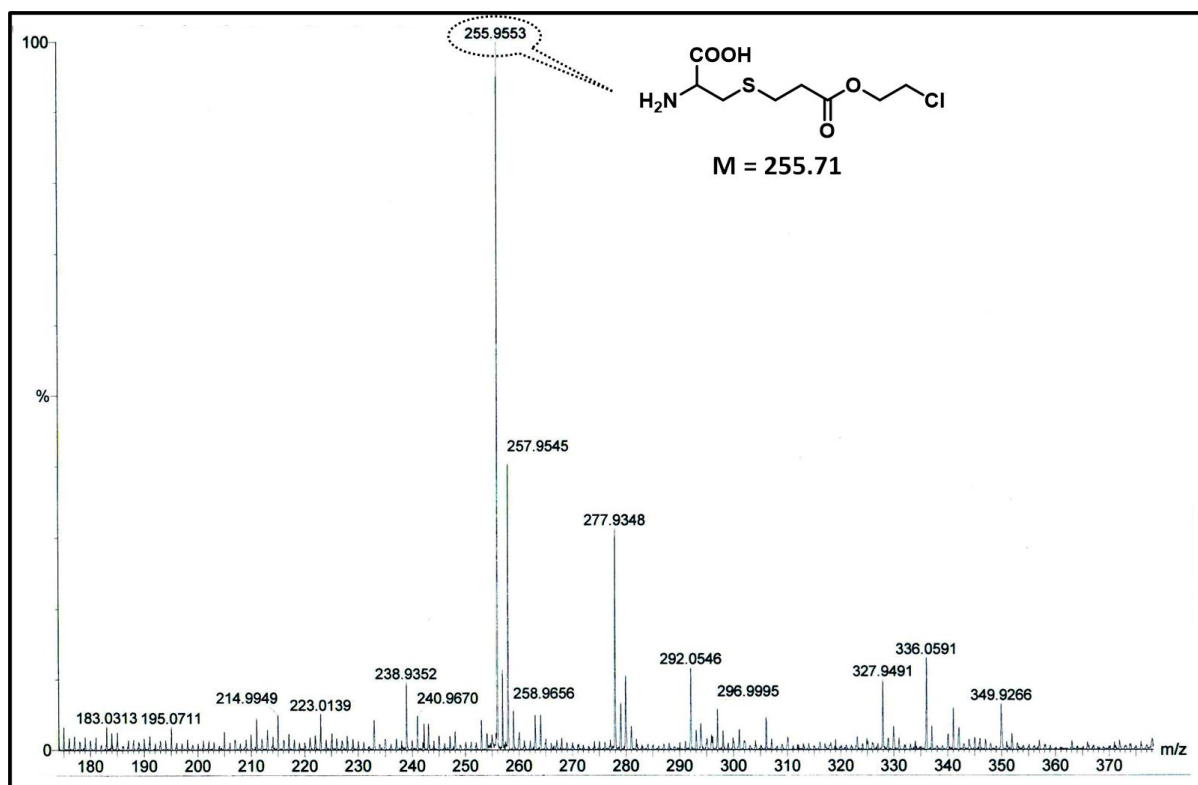
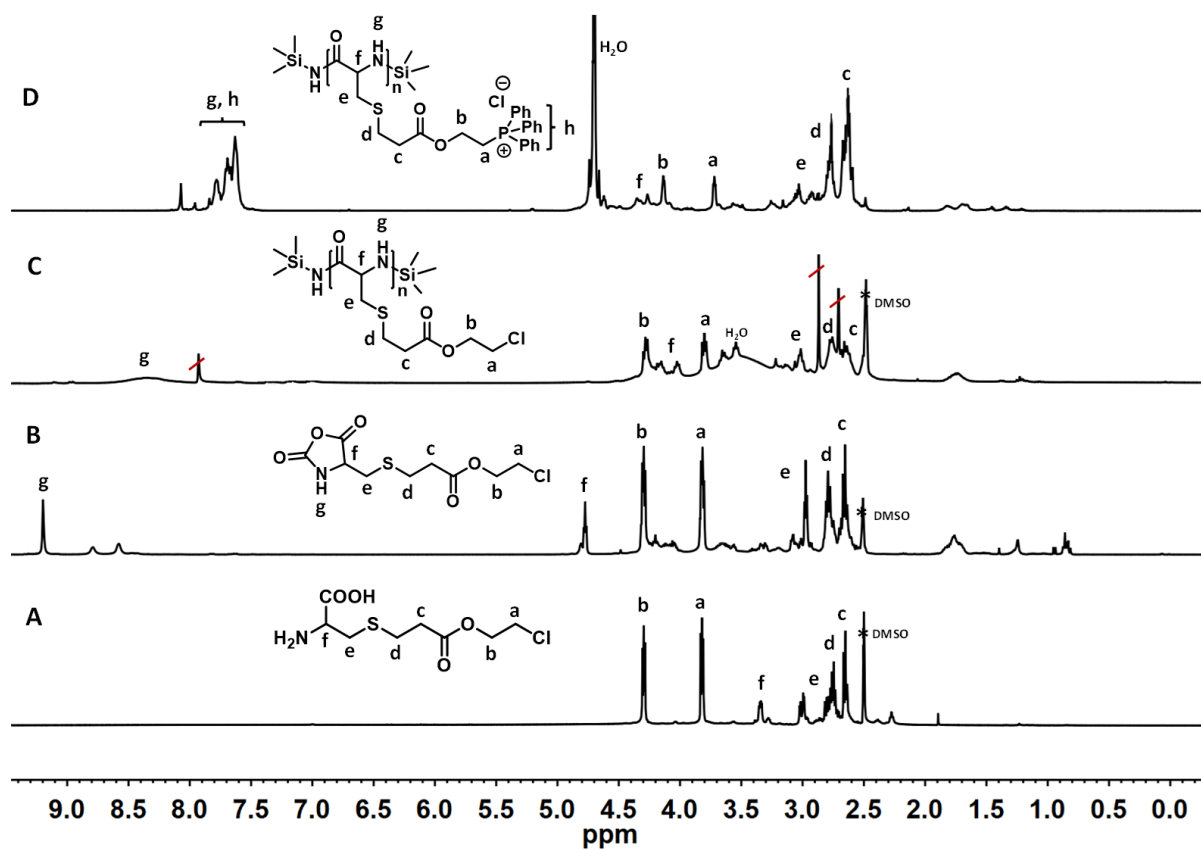


Figure S6.  $^1\text{H-NMR}$  spectrum of Cys-Br in  $\text{D}_2\text{O}$ .



**Figure S7.** ESI-MS spectrum of Cys-Cl in H<sub>2</sub>O: MeOH (1:1) mixture.



**Figure S8.**  $^1\text{H-NMR}$  spectra of Cys-Cl (A), Cys-Cl NCA (B), PCys-Cl (C) in  $\text{DMSO-d}_6$  and  $\text{P}[\text{Cys-PPh}_3]^+[\text{Cl}^-]$  (D) in  $\text{D}_2\text{O}$ .

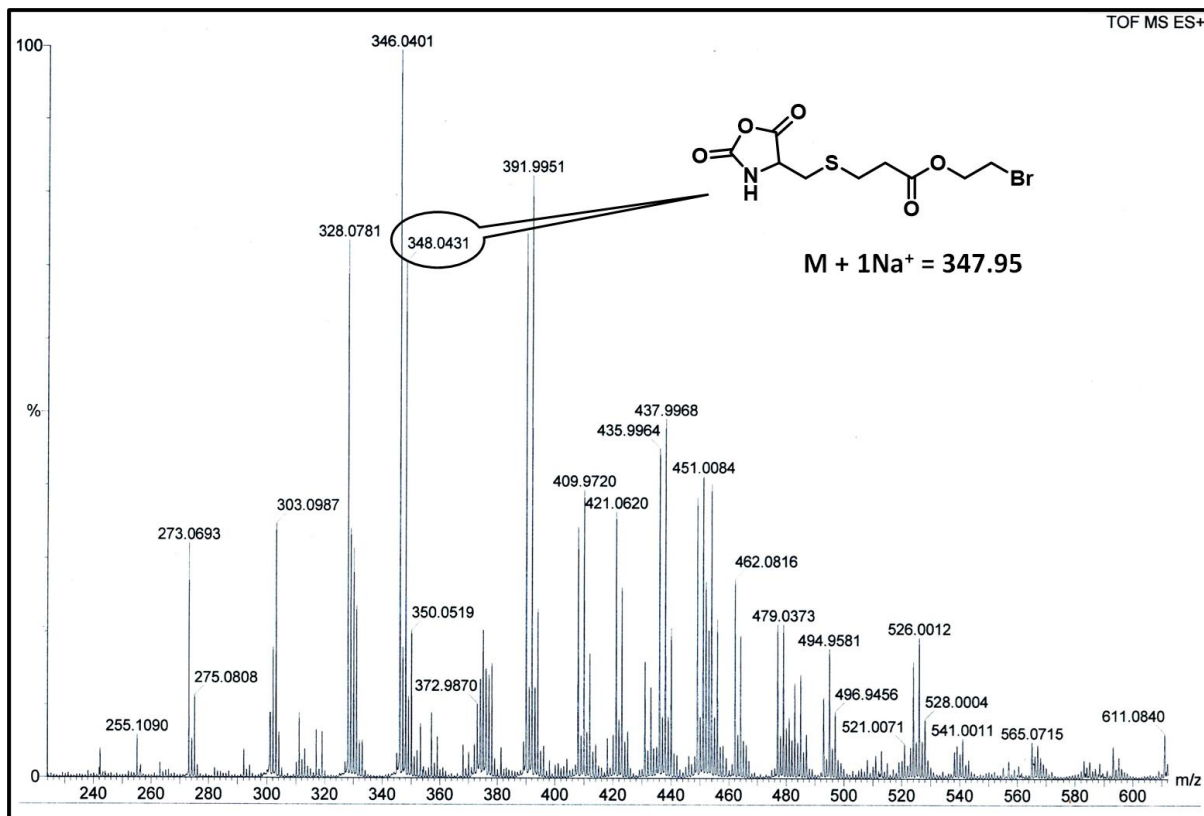


**Figure S9.** ESI-MS spectrum of Cys-Br NCA in DCM.

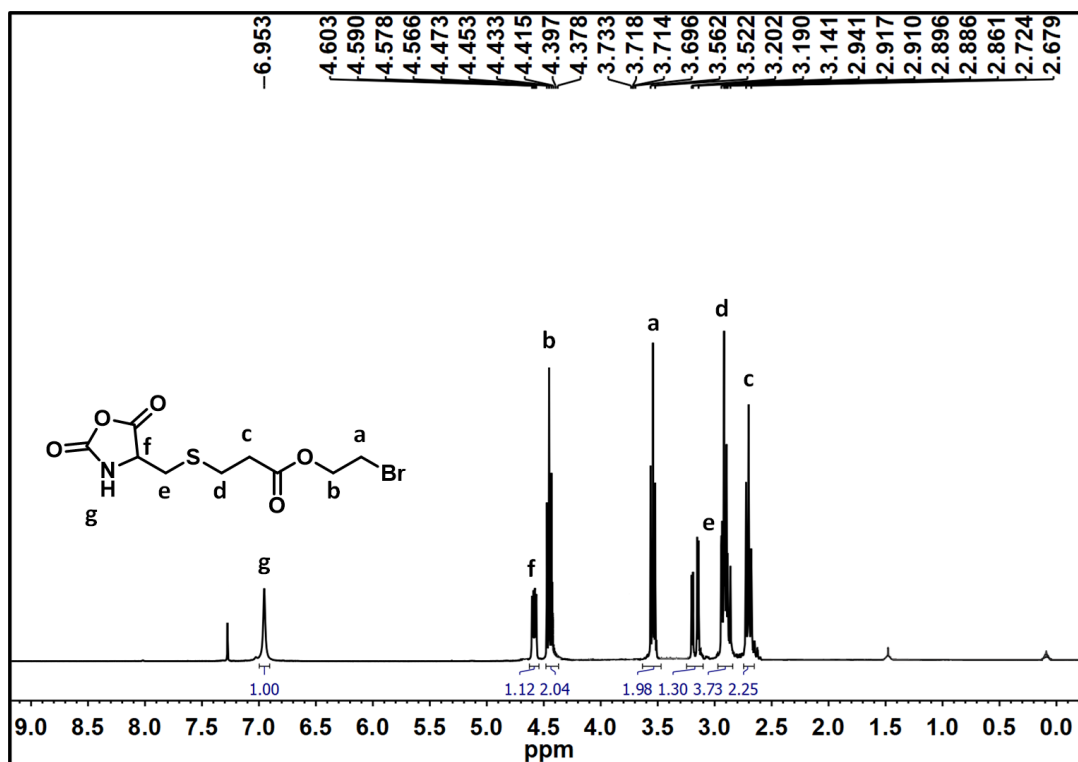


**Figure S10.**  $^1\text{H-NMR}$  spectrum of Cys-Br NCA in  $\text{CDCl}_3$ .

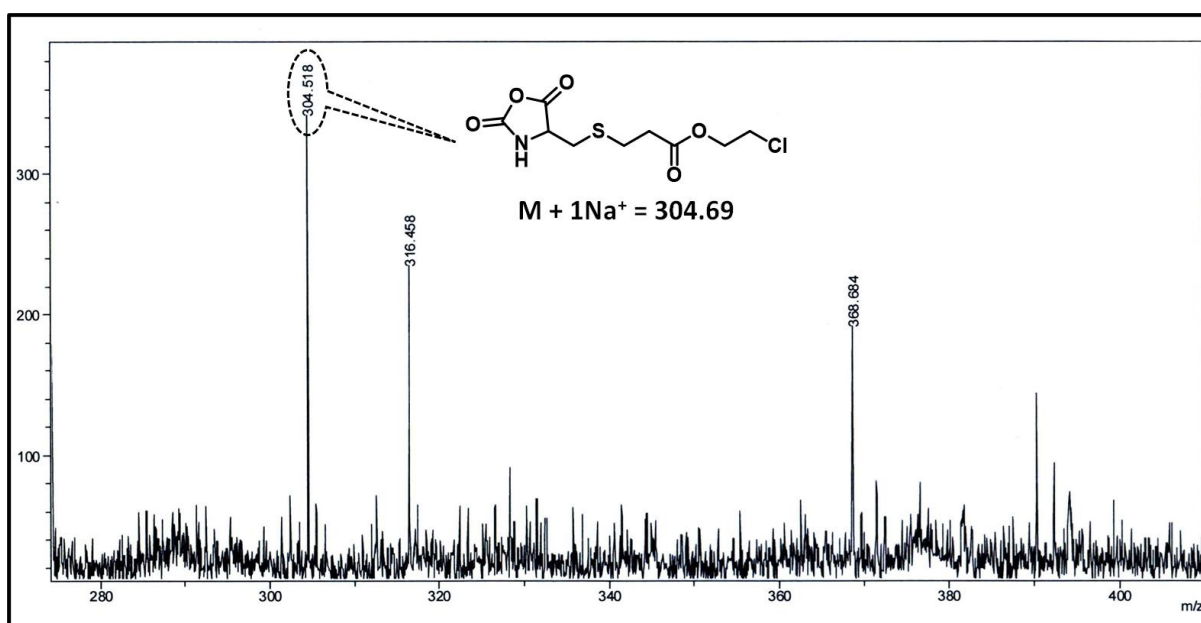


**Figure S11.** MALDI-TOF-MS of Cys-Cl NCA in THF using DCTB matrix and NaI.

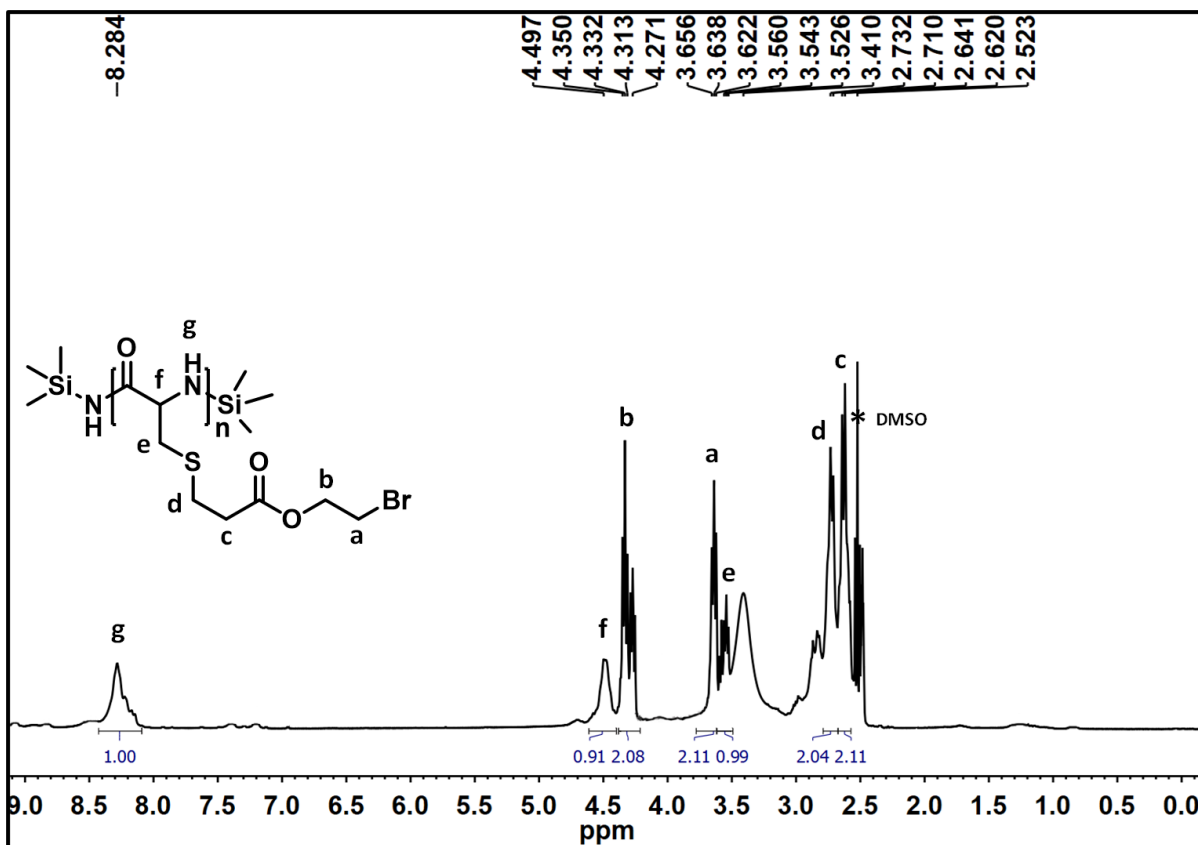


**Figure S12.** <sup>1</sup>H-NMR spectrum of PCys-Br-1 in DMSO-d<sub>6</sub>.

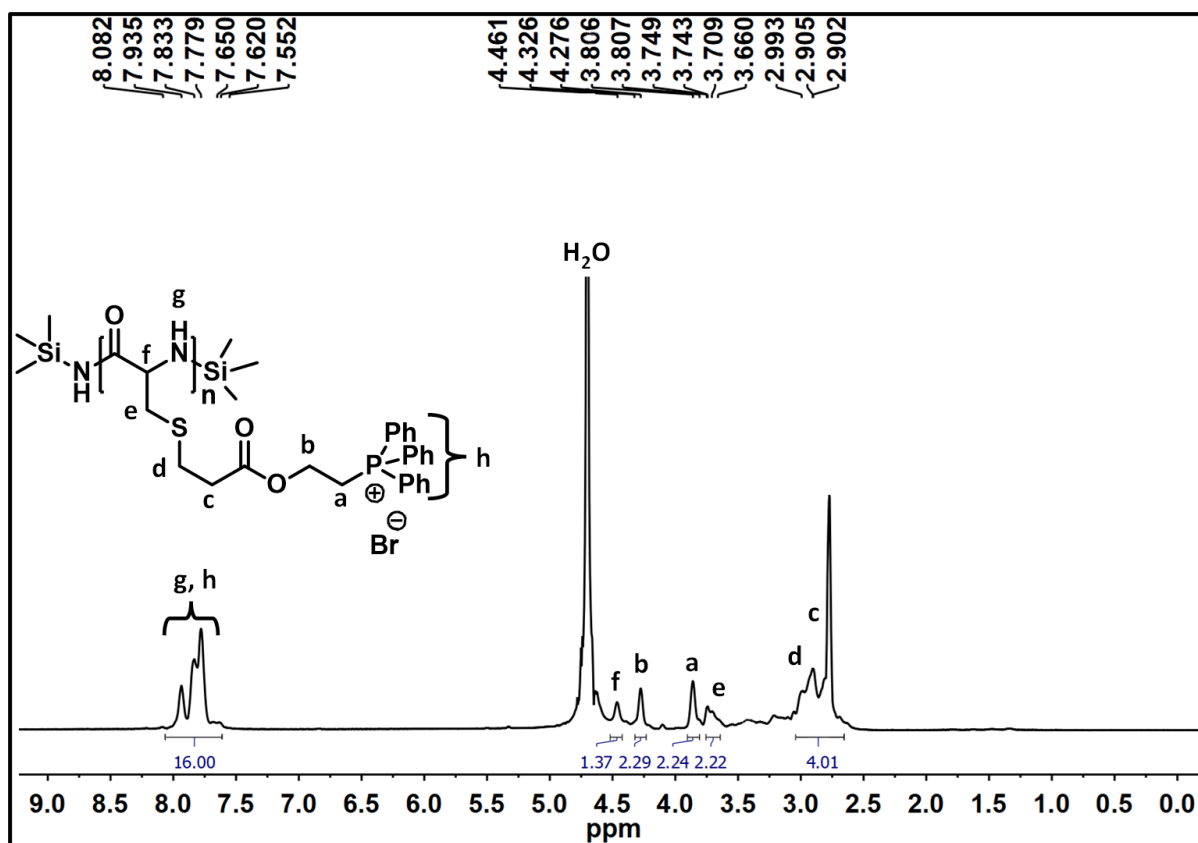


**Figure S13.** <sup>1</sup>H-NMR spectrum of P[Cys-PPh<sub>3</sub>]<sup>+</sup>[Br<sup>-</sup>]-1 in D<sub>2</sub>O.



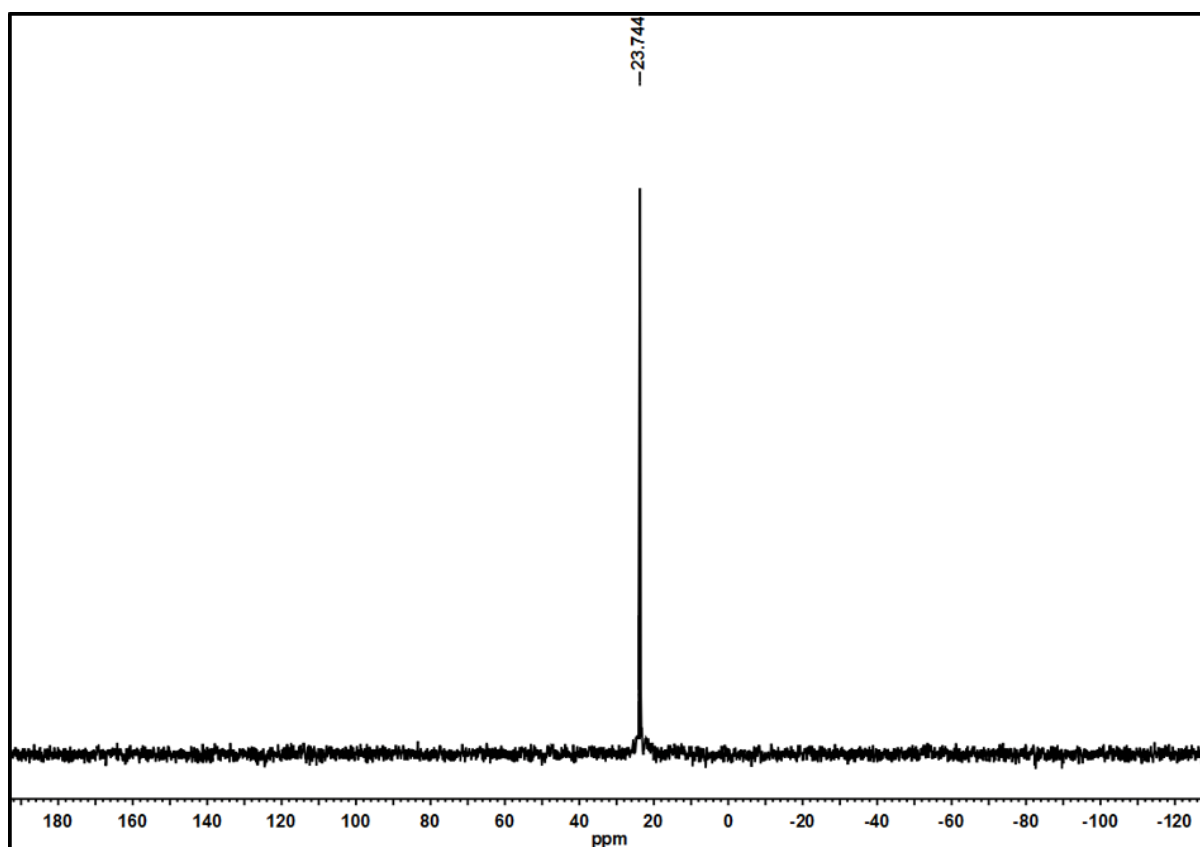


**Figure S14.**  $^{31}\text{P}$ -NMR spectrum of  $\text{P}[\text{Cys-PPh}_3]^+[\text{Br}^-]-1$  in  $\text{D}_2\text{O}$ .

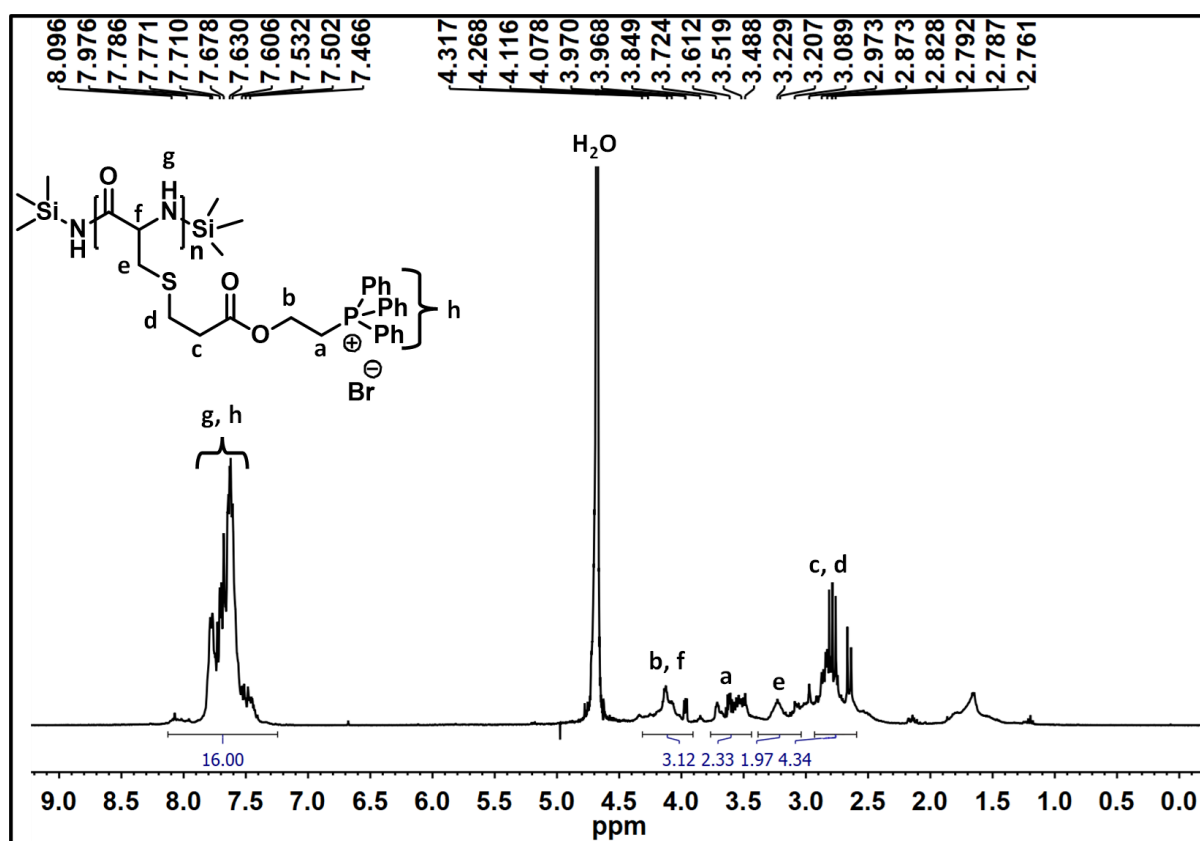


**Figure S15.** <sup>1</sup>H-NMR spectrum of P[Cys-PPh<sub>3</sub>]<sup>+</sup>[Br<sup>-</sup>]<sub>2</sub> in D<sub>2</sub>O.

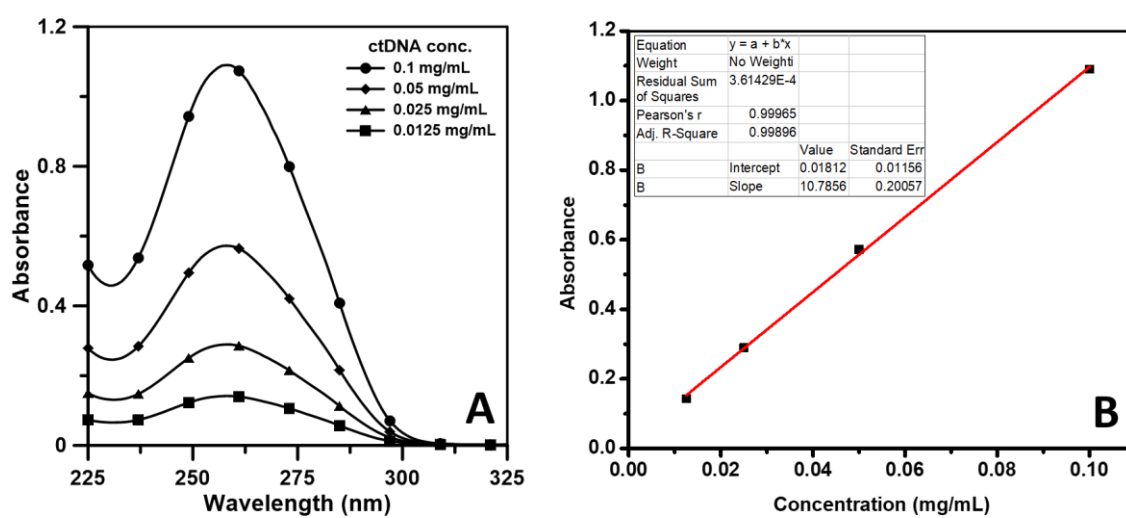


**Figure S16.** UV-Vis absorption spectra of neat ctDNA in Tris-HCl buffer against the variation of its concentration (A). Calibration curve of neat ctDNA in Tris-HCl buffer (B).

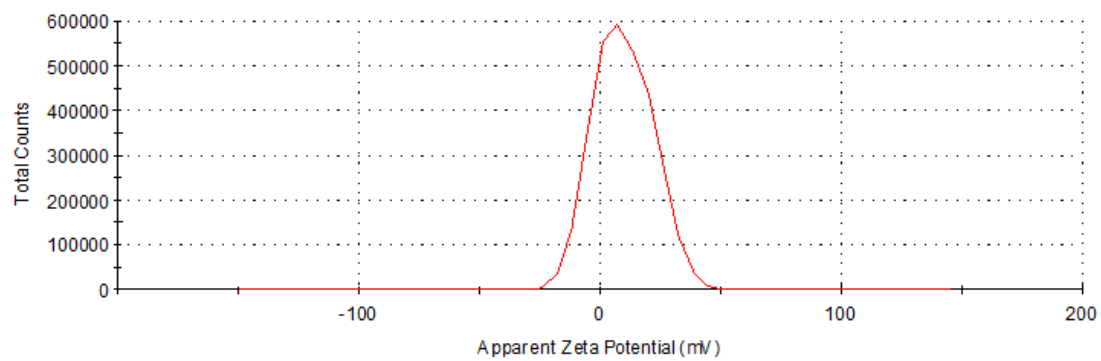


**Figure S17.** Zeta potential ( $\xi$ ) curve of 0.1 wt% P[Cys-PPh<sub>3</sub>]<sup>+</sup>[Br<sup>-</sup>]-1 in H<sub>2</sub>O.

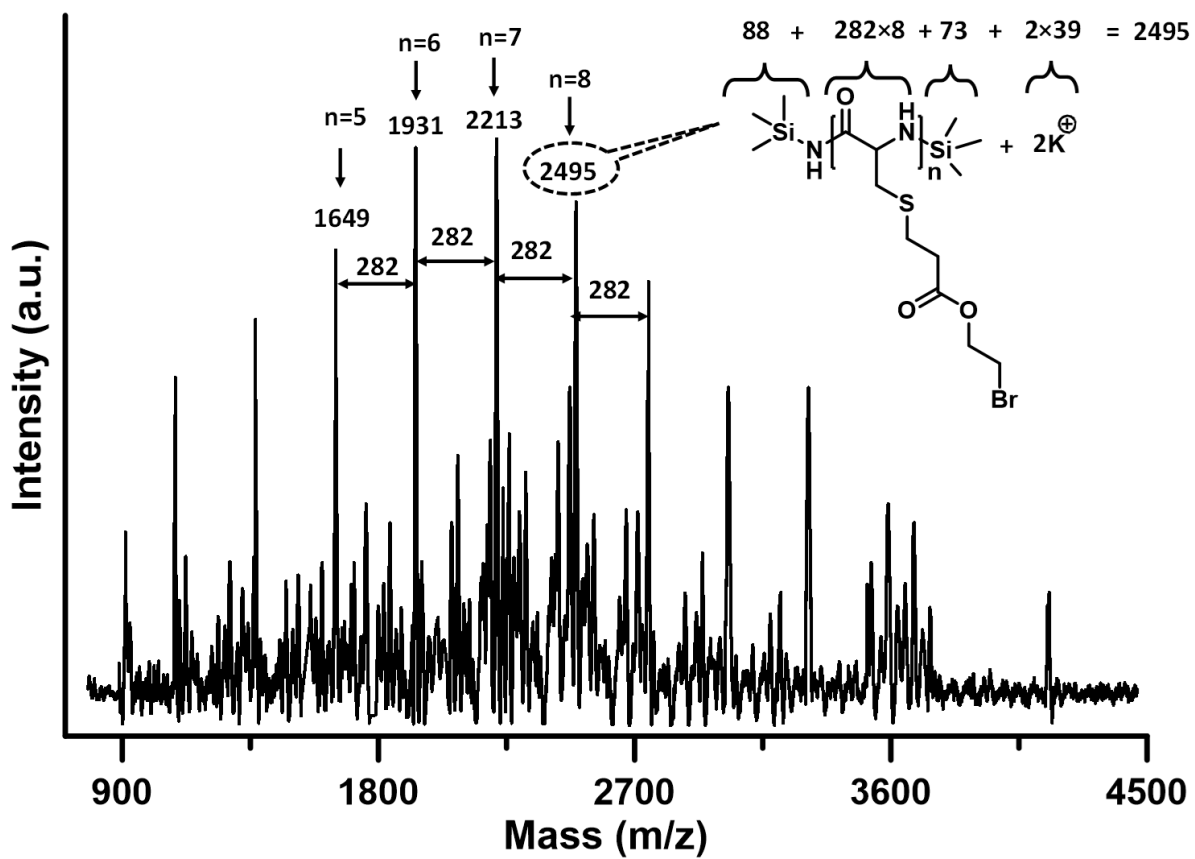


**Figure S18.** MALDI-TOF-MS of PCys-Br-1 in DMF using DHB matrix and NaI.

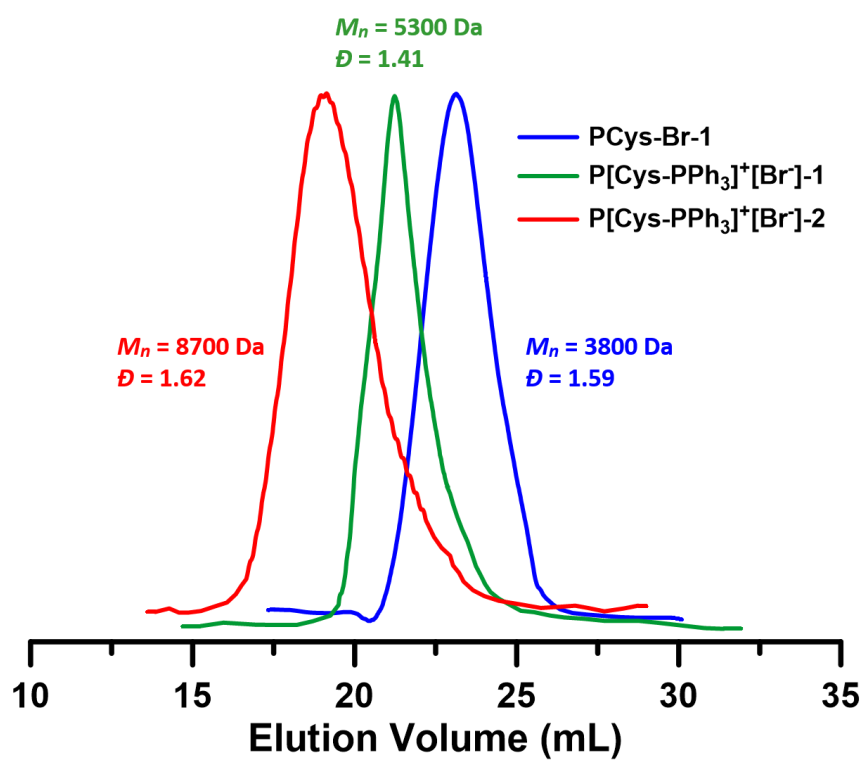


**Figure S19.** SEC chromatograms of PCys-Br-1, P[Cys-PPh<sub>3</sub>]<sup>+</sup>[Br<sup>-</sup>]-1 and P[Cys-PPh<sub>3</sub>]<sup>+</sup>[Br<sup>-</sup>]-2.

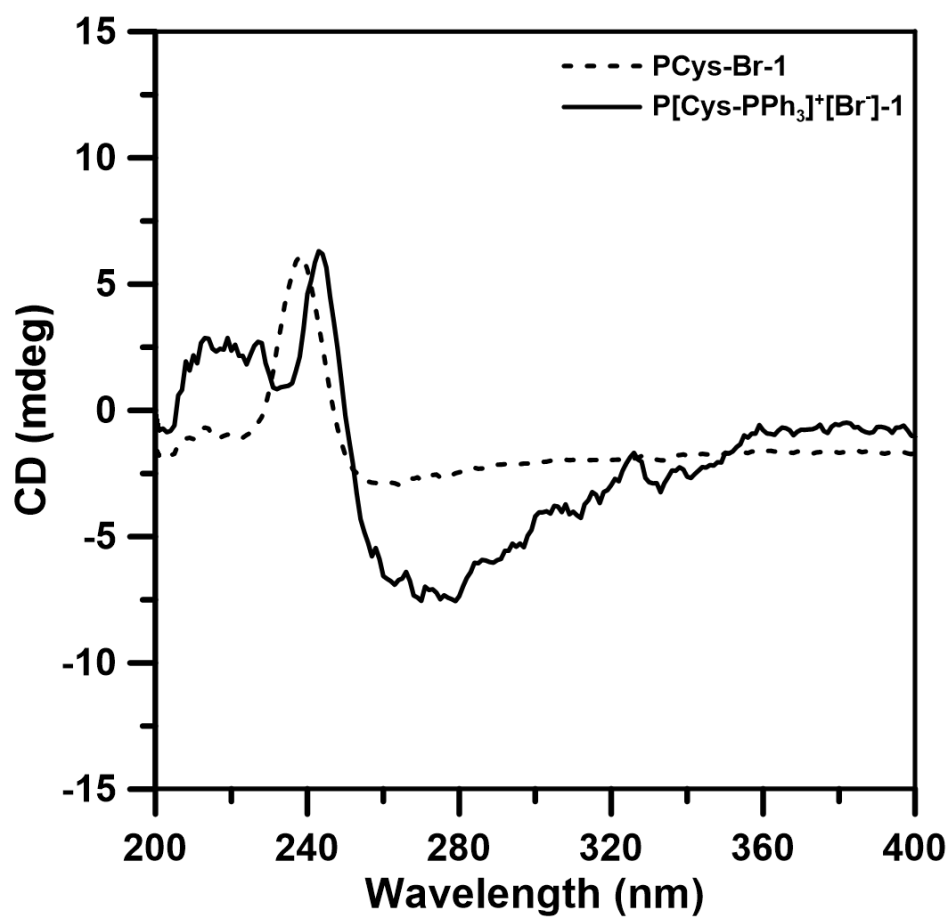


**Figure S20.** CD spectra of PCys-Br-1 and P[Cys-PPh<sub>3</sub>]<sup>+</sup>[Br<sup>-</sup>]-1 showing antiparallel  $\beta$ -sheet like secondary structure.

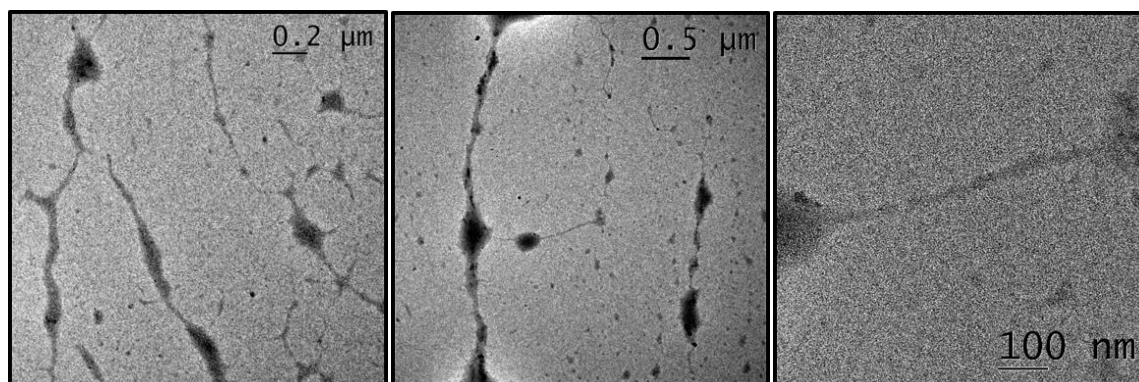


**Figure S21.** TEM image of P[Cys-PPh<sub>3</sub>]<sup>+</sup>[Br<sup>-</sup>]-1(1 mg/mL) in water.



**Table S1.** Sizes of aggregates of P[Cys-PPh<sub>3</sub>]<sup>+</sup>[Br<sup>-</sup>]-1 (0.5 wt%) in the presence of anions in water obtained from DLS experiment

<b>Polypeptide</b>	<b>Anion</b>	<b>[Anion]<sub>min</sub> (mM)</b>	<b><sup>a</sup>D<sub>h</sub> at 25 °C (nm)</b>	<b><sup>b</sup>T<sub>cp</sub> (°C) (DLS) (Heating)</b>	<b>T<sub>cp</sub> (°C) (Turbidity) (Heating)</b>	<b>T<sub>cp</sub> (°C) (Turbidity) (Cooling)</b>
	BF <sub>4</sub> <sup>-</sup>	115	1700	36	39	37
<b>P[Cys-PPh<sub>3</sub>]<sup>+</sup>[Br<sup>-</sup>]-1 (0.5 wt%)</b>	I <sup>-</sup>	65	1200	40	45	47
	ClO <sub>4</sub> <sup>-</sup>	35	850	49	57	57.4
	SCN <sup>-</sup>	15	800	58	66	67

<sup>a</sup> D<sub>h</sub> – Hydrodynamic diameter

<sup>b</sup> T<sub>cp</sub> – Cloud point (data obtained from the temperature-dependent DLS study as shown in Figure S13)

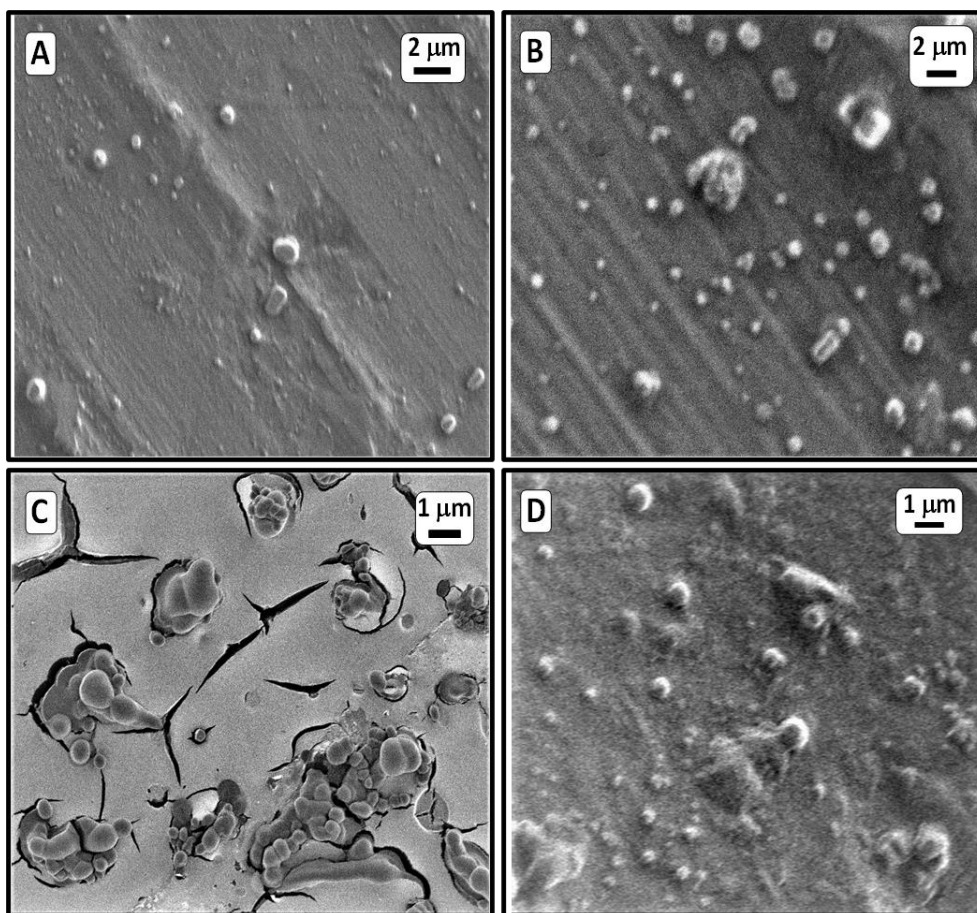


**Figure S22.** FESEM images of P[Cys-PPh<sub>3</sub>]<sup>+</sup>[Br<sup>-</sup>]-1 (0.5 wt%) aggregates in water in the presence of 115 mM BF<sub>4</sub><sup>-</sup> (A), 65 mM I<sup>-</sup> (B), 35 mM ClO<sub>4</sub><sup>-</sup> (C) and 15 mM SCN<sup>-</sup> (D), showing spherical morphologies.

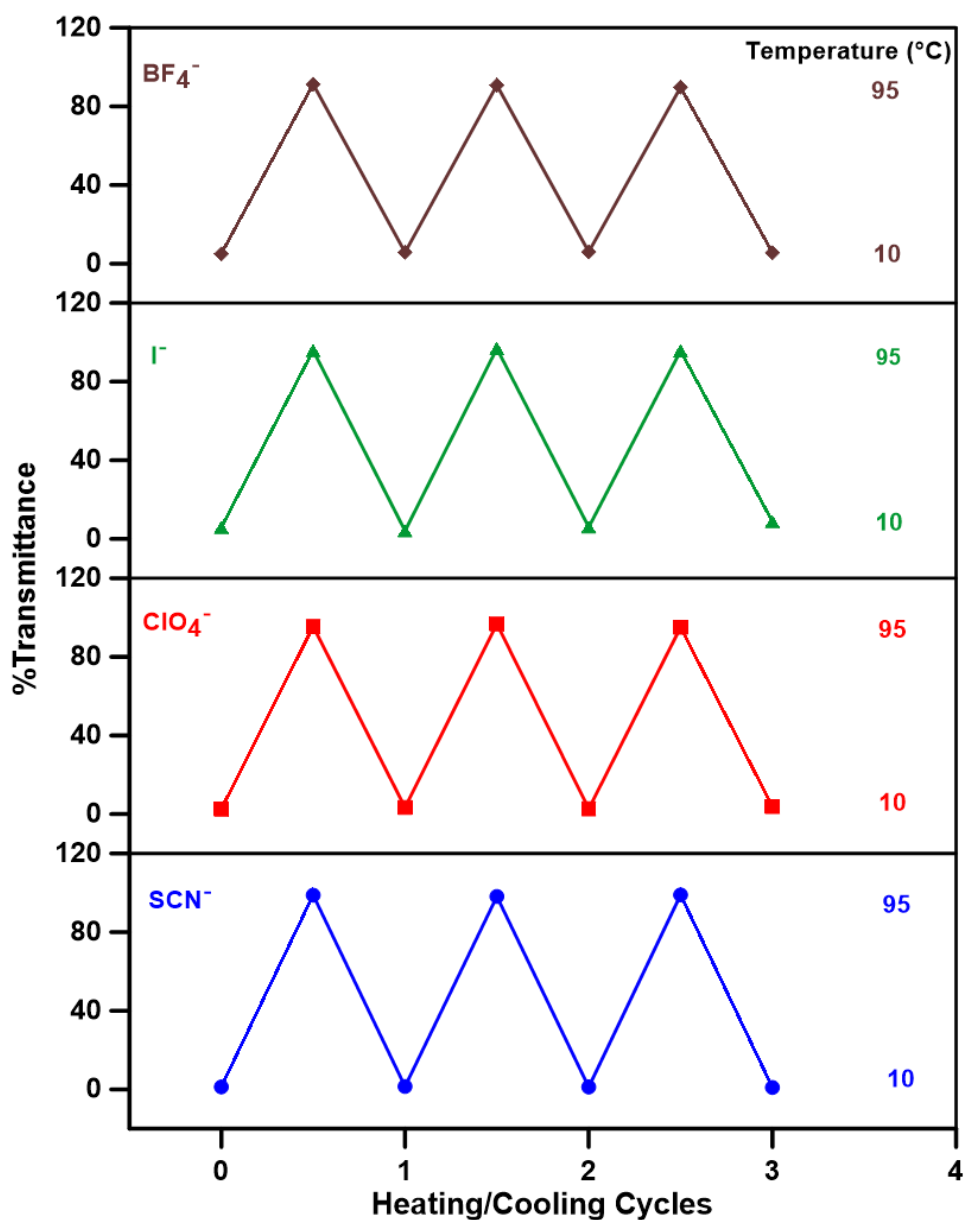


**Figure S23.** Temperature-dependent % transmittance of 0.5 wt% aqueous P[Cys-PPh<sub>3</sub>]<sup>+</sup>[Br<sup>-</sup>]-1 solutions in the presence of different chaotropic anions. Each data point was obtained after equilibrating the corresponding sample solution at the particular temperature for 5 min.

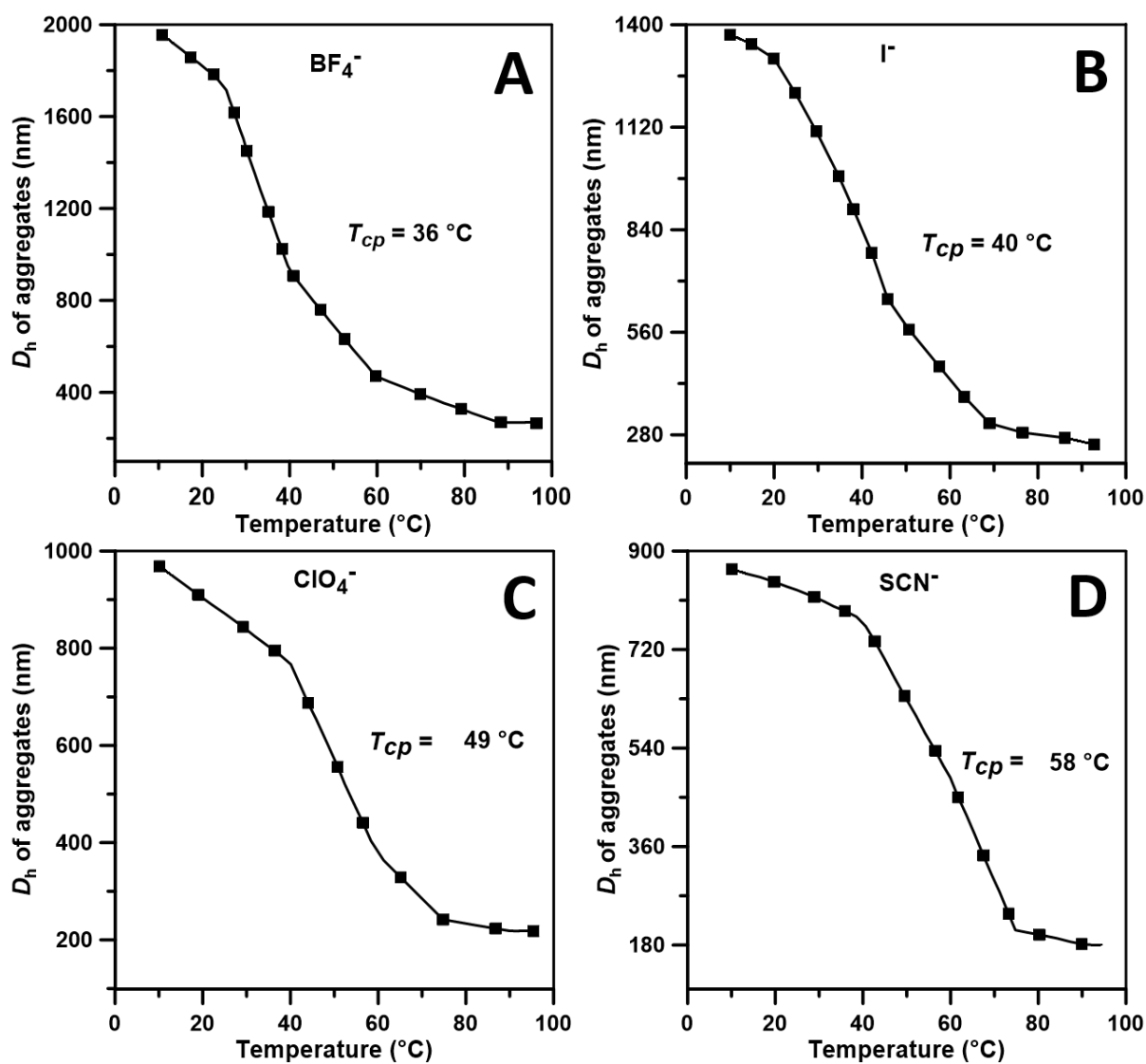


**Figure S24.** Variation of the  $D_h$ s of aggregates of P[Cys-PPh<sub>3</sub>]<sup>+</sup>[Br<sup>-</sup>]-1 (0.5 wt%) in the presence of 115 mM  $\text{BF}_4^-$  (A), 65 mM  $\text{I}^-$  (B), 35 mM  $\text{ClO}_4^-$  (C) and 15 mM  $\text{SCN}^-$  (D) at different temperatures.

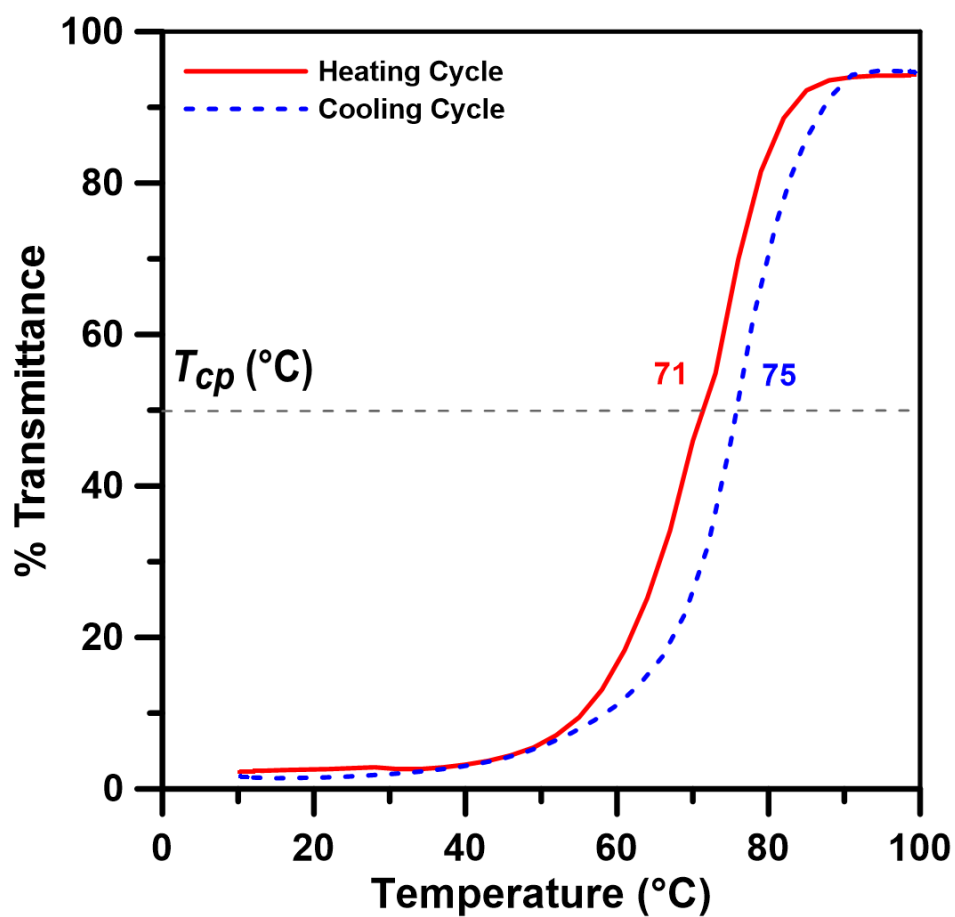


**Figure S25.** Turbidity plot ( $\lambda = 500$  nm) of aqueous P[Cys-PPh<sub>3</sub>]<sup>+</sup>[Br<sup>-</sup>]-2 (0.5 wt%) solution in the presence of 22 mM SCN<sup>-</sup>.

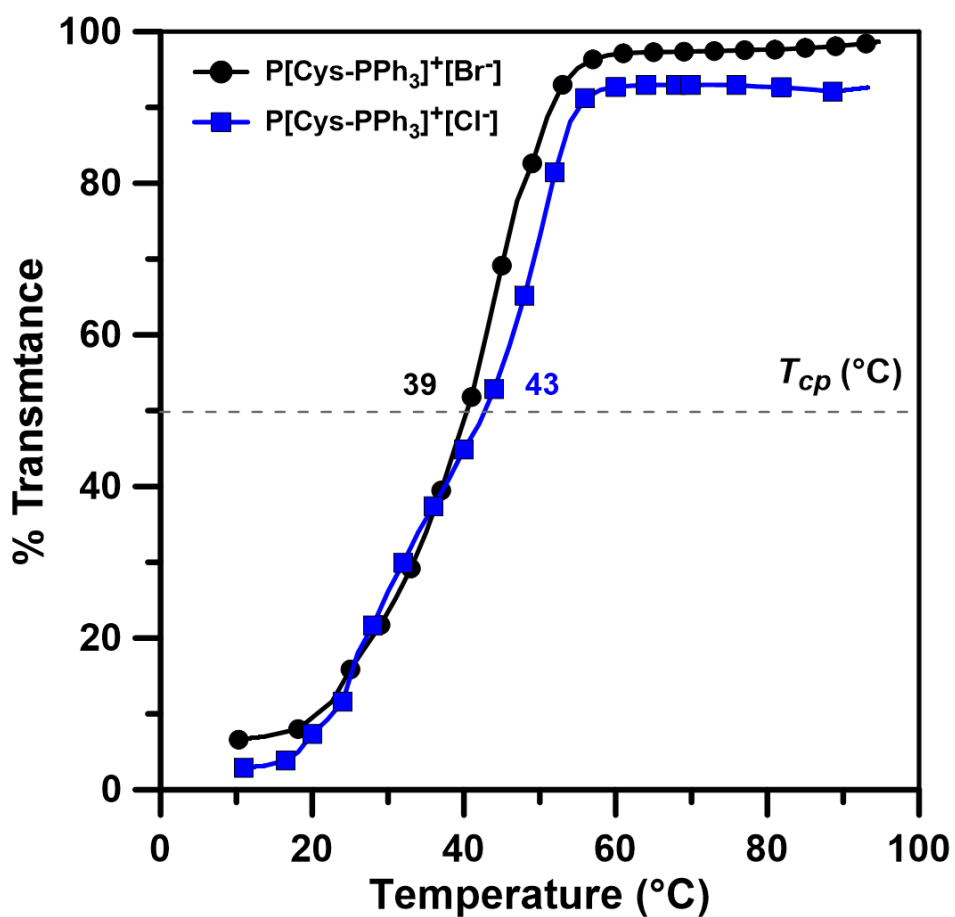


**Figure S26.** Turbidity plot ( $\lambda = 500$  nm) of aqueous P[Cys-PPh<sub>3</sub>]<sup>+</sup>[Br<sup>-</sup>] and P[Cys-PPh<sub>3</sub>]<sup>+</sup>[Cl<sup>-</sup>] (0.5 wt%) solution in the presence of 115 mM BF<sub>4</sub><sup>-</sup>.

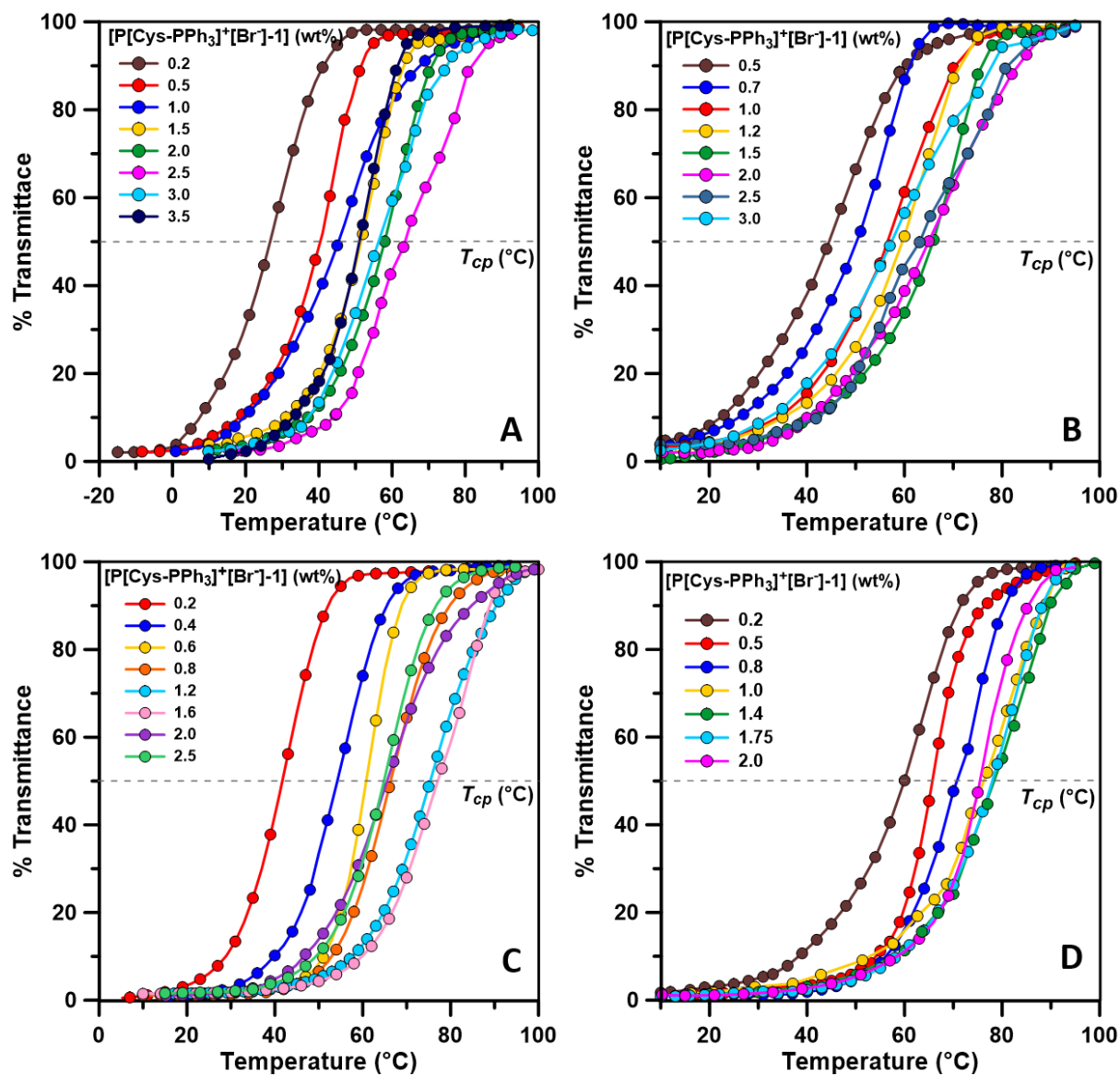


**Figure S27.** Turbidity plots ( $\lambda = 500$  nm) of aqueous P[Cys-PPh<sub>3</sub>]<sup>+</sup>[Br<sup>-</sup>]-1 solutions with varying polypeptide concentration in the presence of 115 mM BF<sub>4</sub><sup>-</sup> (A), 65 mM I<sup>-</sup> (B), 35 mM ClO<sub>4</sub><sup>-</sup> (C) and 15 mM SCN<sup>-</sup> (D).

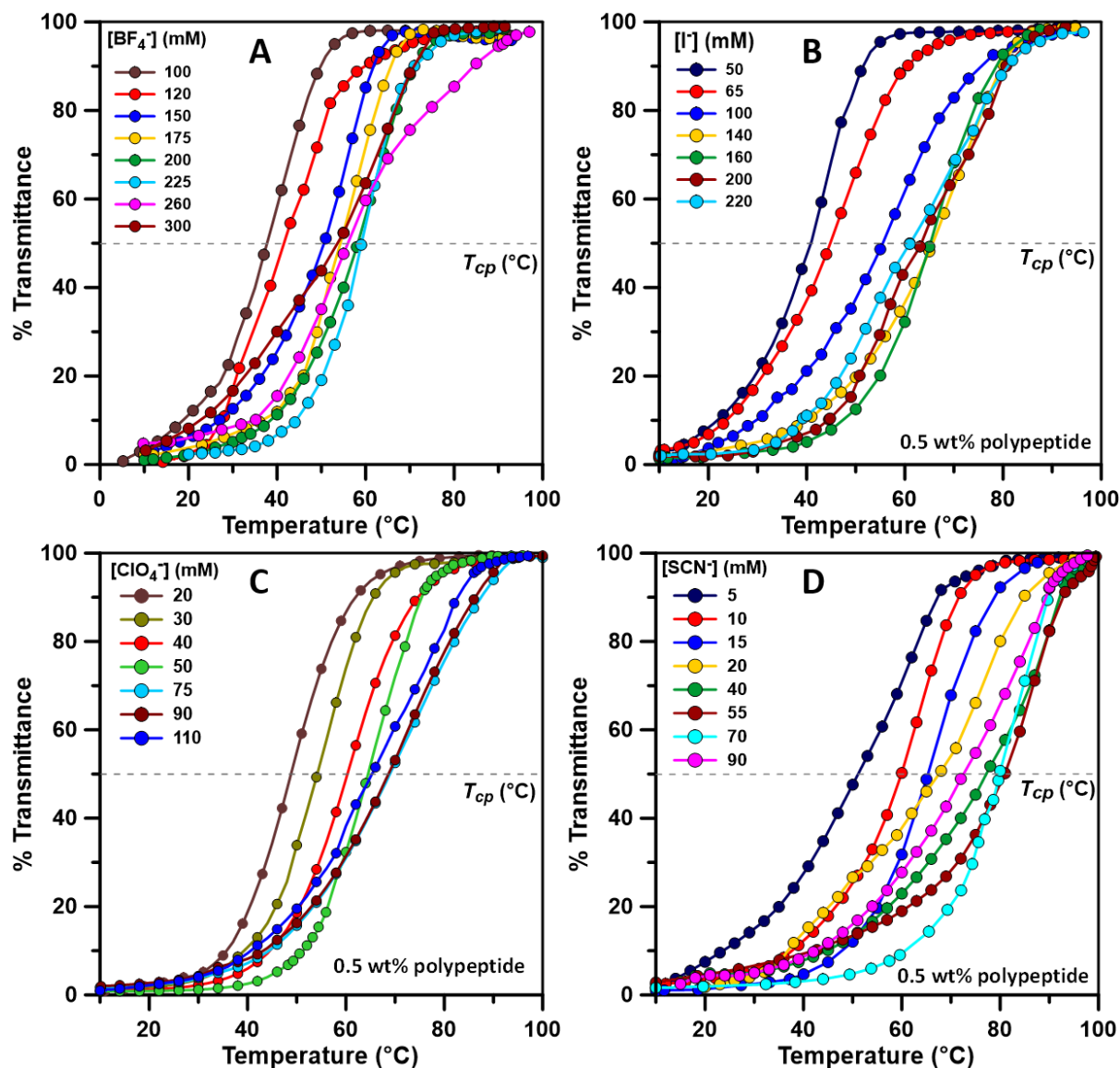


**Figure S28.** Turbidity plots ( $\lambda = 500$  nm) of 0.5 wt% aqueous P[Cys-PPh<sub>3</sub>]<sup>+</sup>[Br<sup>-</sup>]-1 solutions with varying concentration of BF<sub>4</sub><sup>-</sup> (A), I<sup>-</sup> (B), ClO<sub>4</sub><sup>-</sup> (C) and SCN<sup>-</sup> (D).



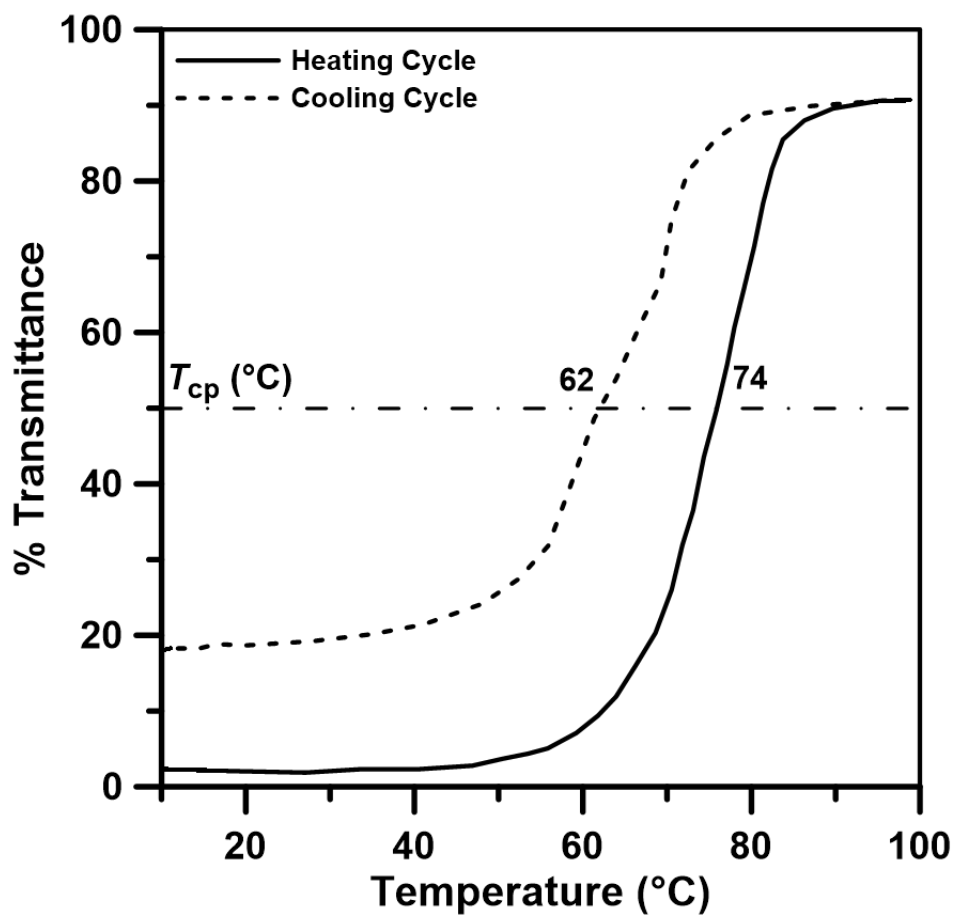


**Figure S29.** UCST-type turbidity curve ( $\lambda = 500$  nm) of 0.5 wt% aqueous solution of P[Cys-PPh<sub>3</sub>]<sup>+</sup>[Br<sup>-</sup>]-1 in the presence of 500 μM of SDS; heating and cooling run showed huge hysteresis.

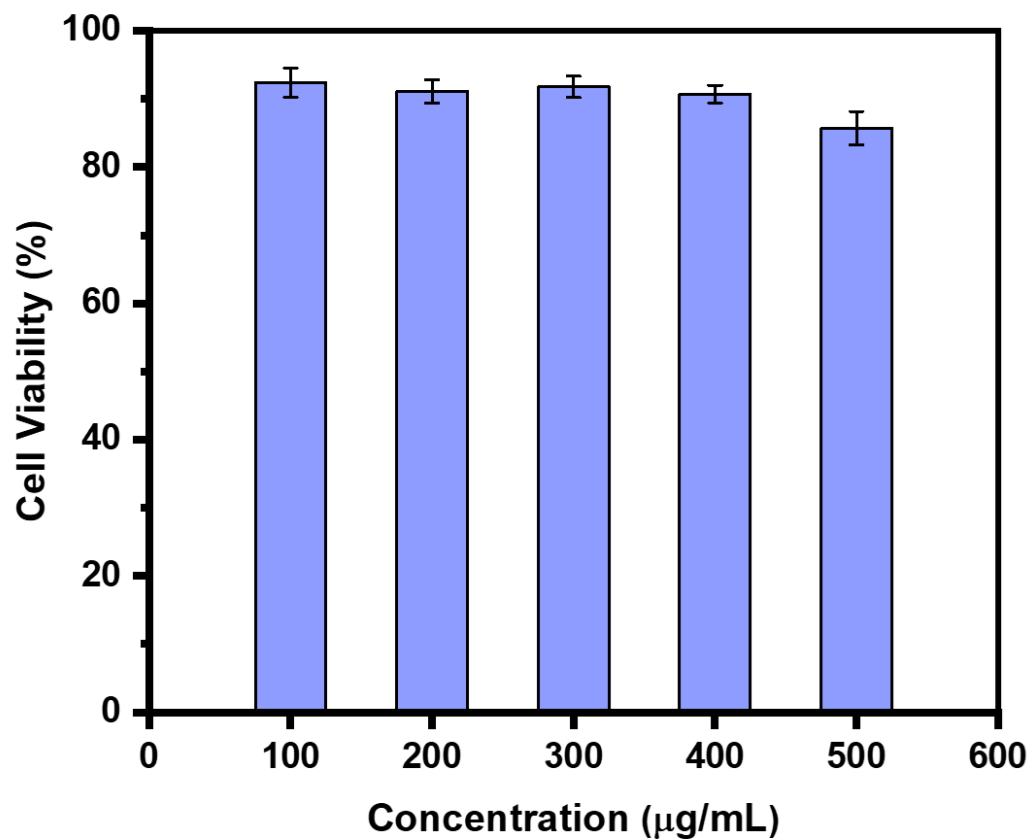
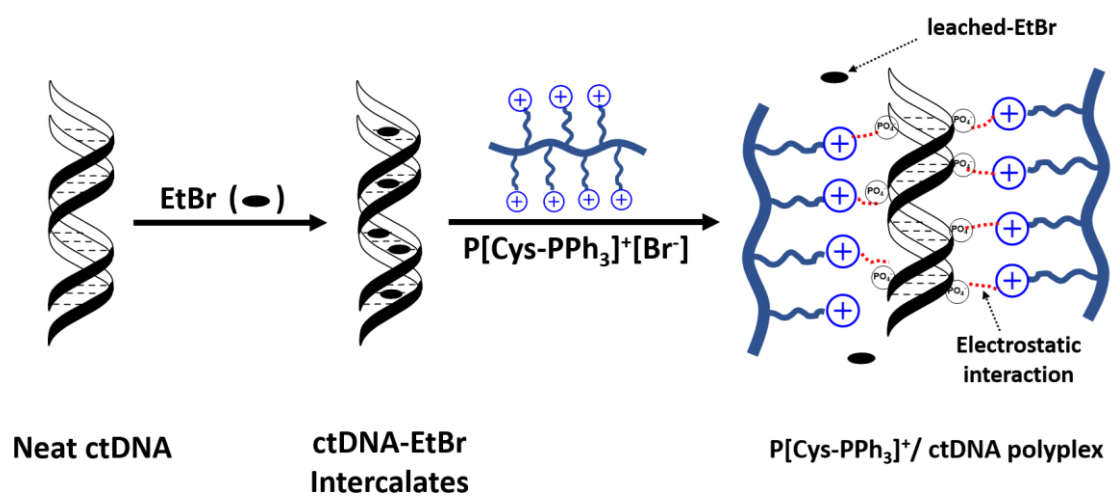


**Figure S30.** The cell viability of KB cells with different concentrations of P[Cys- $\text{PPh}_3$ ] $^+$ [Br $^-$ ]-1 with after 24 h of incubation.



**Scheme S2.** Schematics of polyplex formation of P[Cys-PPh<sub>3</sub>]<sup>+</sup>[Br<sup>-</sup>] with ctDNA in aqueous solution.

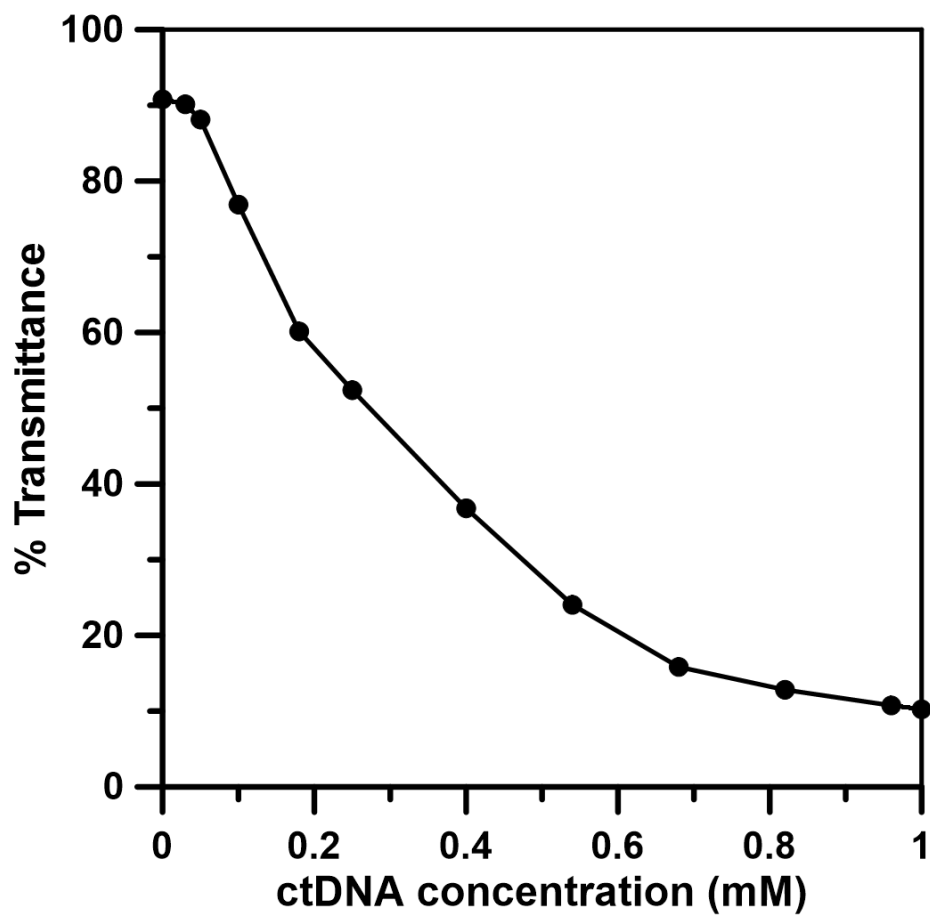


**Figure S31.** Titration plot, showing the % transmittance of 0.5 wt% aqueous P[Cys- $\text{PPh}_3$ ] $^+$ [Br $^-$ ]-1 solution in the presence of different concentration of ctDNA.

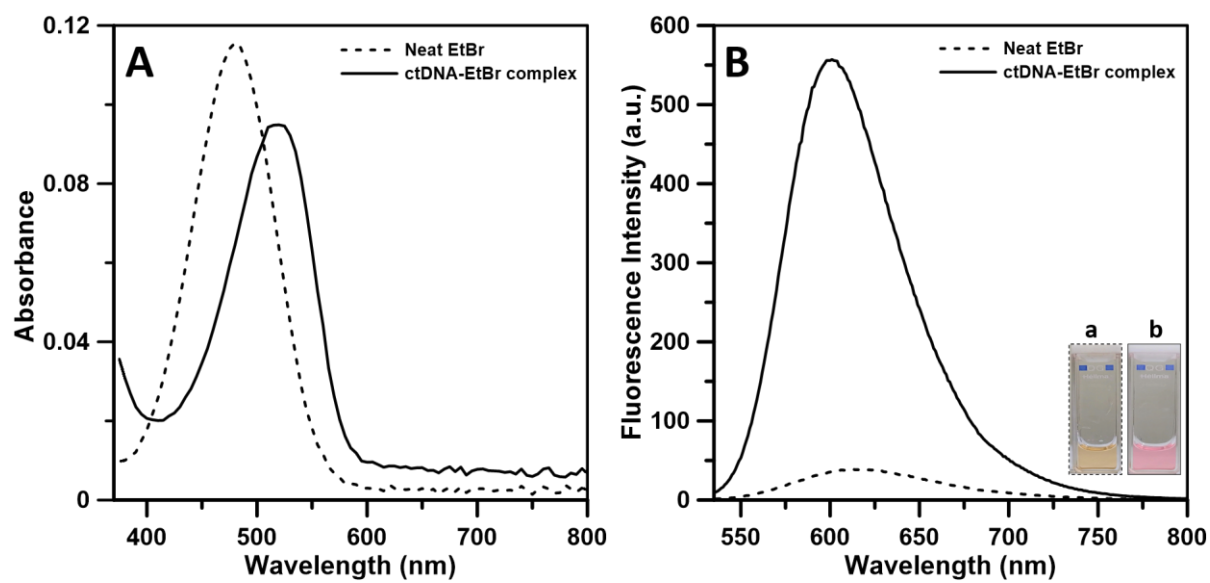


**Figure S32.** Absorption (A) and emission (B) spectra of neat EtBr in water and EtBr-ctDNA complex in Tris-HCl buffer. Inset of the Figure B showed the change in colour of EtBr solution before (a) and after (b) the intercalation with ctDNA.

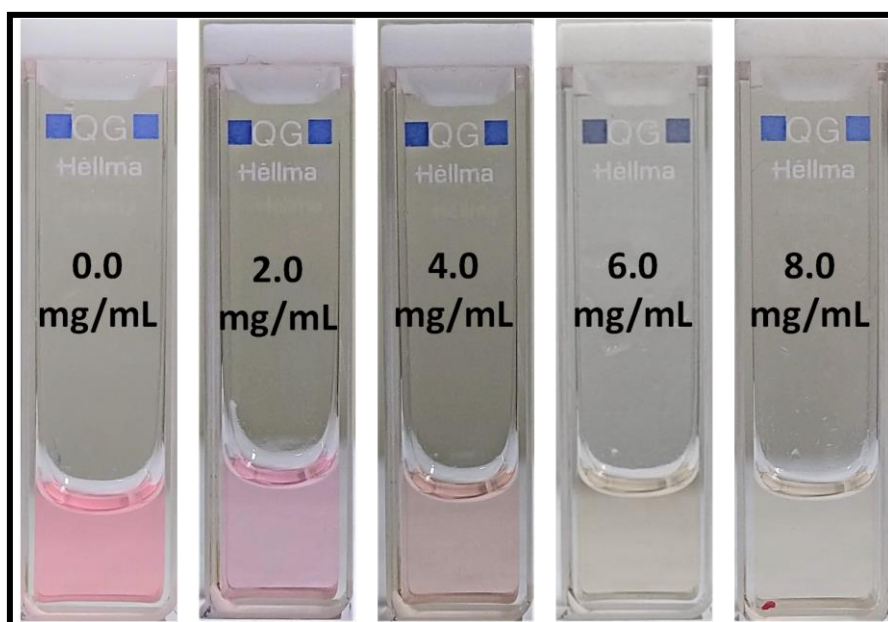


**Figure S33.** Photographs showing the decrease in colour intensity of the ctDNA-EtBr complex with increase in  $P[Cys-PPh_3]^+[Br^-]-1$  concentration in Tris-HCl buffer, indicating the leaching out of EtBr from its intercalated state into the bulk solvent.

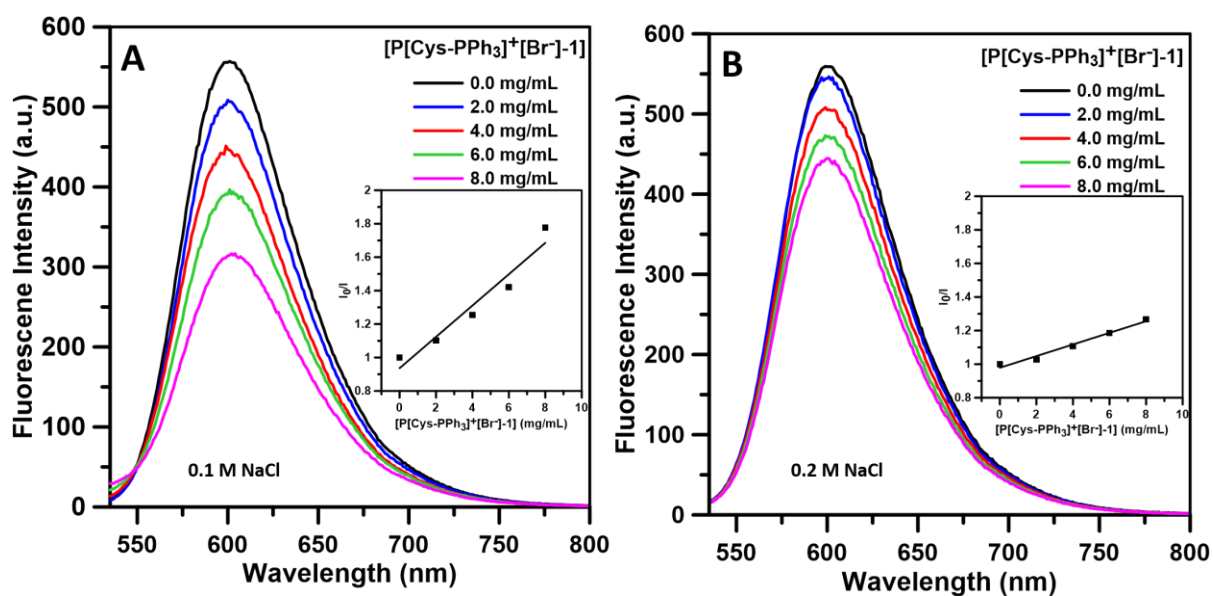


**Figure S34.** Emission spectra of EtBr-ctDNA complex in the presence of different amount of P[Cys-PPh<sub>3</sub>]<sup>+</sup>[Br<sup>-</sup>]-1 with 0.1 M NaCl (A) and 0.2 M NaCl (B) showing the decrease in extent of fluorescence quenching with increase of the ionic strength. The insets of the both figures showed the plot of  $I_0/I$  vs respective [P[Cys-PPh<sub>3</sub>]<sup>+</sup>[Br<sup>-</sup>]-1], revealing the decrease in fluorescence quenching of EtBr-ctDNA complex by P[Cys-PPh<sub>3</sub>]<sup>+</sup>[Br<sup>-</sup>]-1.